Cape Peninsula University of Technology

Development of a radiated emissions test setup for CubeSats

by

PJ Bester
212005952

Completion Date: 14/11/2024
Supervisor: Prof. B. Vipin
Co-Supervisor: Dr. Pieter G. Wiid

Master thesis submitted in fulfilment of CPUT proposal guidelines

Master of Engineering: Electrical Engineering

Abstract

The increasing reliance on CubeSats for both commercial and research applications necessitates rigorous Electromagnetic Compatibility (EMC) testing to ensure mission success and regulatory compliance. Despite their cost-effectiveness, CubeSats missions can be very expensive due to the launch costs. Their susceptibility to Electromagnetic Interference (EMI) can compromise functionality and operational reliability causing mission failure. This research presents a cost-efficient approach to EMC pre-compliance testing tailored to CubeSats, addressing the limitations of existing full-compliance facilities.

The study explores the feasibility of using inexpensive self built Transverse-Electromagnetic (Mode) (TEM) cells, to characterize EMI emissions within CubeSat systems and subsystems. A combination of computational simulations and empirical testing is employed to identify key design parameters influencing the TEM cell performance. Additionally, the impact of component placement and shielding techniques on interference mitigation is examined.

Experimental results validate the accuracy and range of the proposed methodology in detecting and mitigating EMC anomalies before launch, thereby reducing the risk of mission failure due to interference-related issues. The findings contribute to the standardization of affordable pre-compliance EMC testing protocols, enabling broader access to space technology for emerging players in the industry. Furthermore, recommendations are provided for integrating EMC considerations early in the CubeSat design process, ensuring improved reliability and performance.

Acknowledgements

The author thanks Cape Peninsula University Of Technology (CPUT) and the technical staff for their assistance in manufacturing the TEM cell components. Thank you to Prof. B. Vipin, and Mr. B. Williams for their support and assistance without whom this project may not have come to fruition. A very special thanks to Dr. Pieter G. Wiid without who's guidance, support, assistance and expertise this project would not have been possible

Contents

List of Figures

Acronyms & Abbreviations

CEN Comité Européen de Normalisation.

CG Comb Generator.

CISPR Comité International Spécial des Perturbations Radioélectriques.

CPUT Cape Peninsula University Of Technology.

CTSL Coax To Stripline.

DUT Device Under Test.

ECSS European Cooperation for Space Standardization.

EM Electromagnetic.

EMC Electromagnetic Compatibility.

EMI Electromagnetic Interference.

F'SATI French South African Institute Of Technology.

FCC Federal Communications Commission.

GTEM Gigaherz Transverse-Electromagnetic (Mode).

IEC International Electrotechnical Commission.

ISO International Organization for Standardization.

LUF Lowest Usable Frequency.

PCB Printed Circuit Board.

RBW Resolution Bandwidth.

RE Radiated Emissions.

RS Radiated Susceptibility.

STWS Strip To Wide Stripline.

TEM Transverse-Electromagnetic (Mode).

VNA Vector Network Analyzer.

Chapter 1

Introduction

1.1 Background

1.1.1 F'SATI

In recent years, the French South African Institute Of Technology (F'SATI) has emerged as a key player in the South African space industry, having successfully launched and operated multiple CubeSats ((F'SATI 2021a), (F'SATI 2021b), (Boyce 2021)). The organisation has also made significant contributions to antenna, transmitter, and transceiver development, positioning itself as a leader in a new space paradigm, where educational institutions and smaller organisations have increasing access to space technology that was previously limited to large agencies and corporations. Although CubeSats have traditionally been used for demonstrations of technology and research purposes, adherence to EMC requirements has been absent. However, with the growing number of commercial applications and the increasing dependence on CubeSat technology, proper EMC testing have become a necessity. To address this need, this project aims to develop a robust test set-up that will ensure cost-effective EMC pre-compliance testing for CubeSats.

1.1.2 CubeSats

CubeSat missions can have relatively large budgets, despite being primarily used by students, researchers, and universities, with launch costs ranging from 180,000 to 250,000 USD for a 3U CubeSat (Rocker Lab USA 2020). Therefore, proper EMC testing is critical to prevent CubeSats from becoming space debris orbiting Earth. The Wake Shield experiment is a cautionary tale documented in NASA Reference Publication 1374 (R.D. Leach 1995) where the experiment failed due to inductive coupling between an unshielded attitude control sensor cable and the power bus of the spacecraft. Had adequate EMC testing been conducted on time, the problem could have been resolved with minimal extra cost. With CubeSats similar EMC issues could arise, thereby requiring EMC testing to improve the reliability of CubeSat missions (**RQ1 p.11**). As Keith Williams noted in his book *EMC for Systems and Installations*, interference between neighbouring devices is a function of the distance that separates them (Armstrong 1999). The CubeSat standard, which limits the size and shape of the satellite, and thus the placement of PCBs, creates an environment with a high risk of EMI, which poses a substantial threat to EMC. Figure 1.1 illustrates typical PCB placement in CubeSats and the short distances between the different subsystems[1].

[1]The CubeSat as a whole is seen as a system and the PCB's that make up this system in its entirety each form part of it and is therefore referred to as the various subsystems.

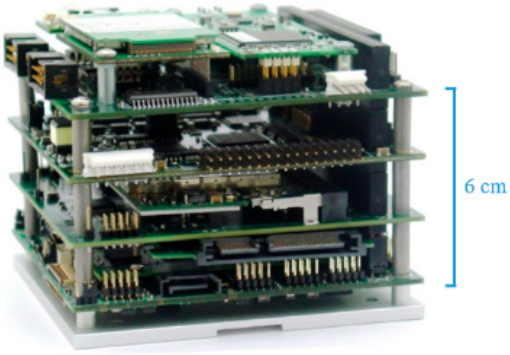

Figure 1.1: CubeSat with PC104 type stackable PCB's (Diamond Systems 2021)

1.1.3 EMC

The concept of EMC refers to the ability of a device to function correctly in its intended electromagnetic environment as well as keeping it's Electromagnetic (EM) noise with an acceptable margin of error (IEEE Std 1302-2019 2020). EMC is an important consideration in the design and operation of electronic devices, as EMI can cause malfunctions or even failures of electronic systems. To ensure EMC, devices must be designed to limit their electromagnetic energy emissions and be immune to external electromagnetic disturbances. EMC testing and certification are mostly required by regulatory agencies to ensure that electronic devices meet established standards for electromagnetic emissions and immunity.

1.2 Research Problem

To ensure the success of CubeSat missions, it is crucial that F'SATI perform the appropriate EMC testing. To achieve this, F'SATI could collaborate with other institutions that possess EMC testing capabilities or invest in their own equipment and facilities to provide pre-compliance testing capabilities. As CubeSats become increasingly complex, the need for appropriate EMC tests will continue to grow (Sibanda and Van Zyl 2016). Therefore, F'SATI should consider taking measures to ensure the success of future CubeSat missions.

1.3 Research Motivation

EMC Testing and CubeSat Design Improvement

EMC testing improves CubeSat mission reliability by identifying and mitigating EMI and other EMC issues early in the design phase. This ensures pre-compliance with standards, reducing the risk of subsystem interfering with one another.

Mission-Specific Testing Factors

Payload configurations differ depending on the CubeSat missions and can affect a variety of parameters such as communication frequencies, power distribution systems, operational environments, subsystem density and system size. Wherefor with depending on the mission parameters, CubeSats vary greatly in complexity and influence the testing methodology and requirements for CubeSat missions and by extension the testing required for EMC. Thereby requiring a versatile cost effective EMC pre-compliance testing solution.

Necessity of Subsystem-Level Testing

Subsystem-level testing is crucial for ensuring overall EMC and performance. Interactions between subsystems can introduce new EMI sources, and subsystem-level testing identifies and helps resolves these issues during the design and development phase, enhancing mission reliability.

Benefits of On-Site EMC Test Equipment

On-site EMC test equipment allows for real-time testing, validation, and optimization of CubeSat subsystems during development. It reduces dependency on external testing services, saving time and costs, and enhances project control to ensure compliance with EMC requirements from inception to deployment.

1.4 Research Objectives

The objective is to develop an in-house cost-effective test set-up for EMC pre-compliance testing, which plays a vital role in CubeSat design and implementation. The proposed setup aims to facilitate the quantification of pre-compliance data for CubeSat subsystems, with a particular focus on Radiated Emissions (RE). This entails investigating and implementing specific test specifications tailored to CubeSat requirements. Integrating RE tests into the CubeSat design methodology is expected to yield design improvements during the early stages, leading to cost savings and enhancing overall mission success prospects.

1.5 Research Questions

RQ1 **How will EMC testing improve the CubeSat design process?**
Objective: To enhance CubeSat mission reliability by identifying and mitigating potential electromagnetic interference issues early in the design phase, ensuring pre-compliance, and minimizing the risk of interference with the CubeSat subsystems.

RQ2 **What other equipment and instrumentation are needed for EMC tests on CubeSat subsystems?**
Objective: To determine the additional equipment required for comprehensive EMC testing, including a spectrum analyser or oscilloscope, a coaxial cable with an N-type connector, and E and H-field probes to assist in pinpointing causes of EMI on PCBs for targeted redesign efforts.

RQ3 **How will the tested equipment and the developed methodology be verified?**
Objective: To validate the developed equipment and methodology by generating known frequency values using a comb generator and comparing the measured values in the built TEM cell with the expected frequencies to ensure they are within an acceptable range.

RQ4 **What are the benefits of having this type of test equipment on site?**
Objective: To enable real-time testing, validation, and optimization of CubeSat subsystems during development, reducing the need for outsourcing testing services, saving time and costs, and enhancing project control to ensure CubeSat missions meet EMC requirements from inception to deployment.

RQ5 **How does the TEM cell compare to other more expensive testing facilities such as reverberation chambers**

Objective: To asses that accuracy and thereby determine the usability of the TEM cell as in-expensive EMC pre-compliance test equipment.[2]

RQ6 **What is the frequency range of the TEM cell?**
Objective: To understand which equipment can be tested and up to what frequency while still retrieving reliable information.

RQ7 **What are the costs of the currently available EMC testing solutions?**
Objective: To analyse and document the cost structure of existing electromagnetic compatibility (EMC) testing solutions, identifying price ranges and the factors influencing these costs to provide a benchmark for in-house alternatives.

RQ8 **Which solutions are the most suitable for an in-house testing facility?**
Objective: To evaluate and compare various EMC testing solutions based on technical requirements, space constraints, and cost-effectiveness, with the goal of identifying optimal solutions for implementation in a small-scale, in-house testing facility.

RQ9 **How do you design an open TEM cell?**
Objective: To develop a detailed design methodology for constructing an open transverse electromagnetic (TEM) cell, including the theoretical and practical considerations necessary to achieve a reliable setup for EMC testing.

RQ10 **Which parameters can be optimized for improved performance?**
Objective: To identify and analyze the key design parameters of a TEM cell that impact performance, such as field uniformity, cell dimensions, and materials, and propose optimization techniques to enhance testing accuracy and efficiency.

RQ11 **How do you verify a TEM cell to qualify for pre-compliance EMC testing before starting manufacturing?**
Objective: To establish a verification protocol for ensuring that the designed TEM cell meets pre-compliance EMC testing standards before spending capital on the manufacturing.

RQ12 **How does such a solution compare to available off-the-shelf TEM cells with respect to performance and cost?**
Objective: To conduct a comparative analysis of the custom-designed TEM cell against commercially available options, focusing on differences in performance metrics, compliance with EMC standards, and cost savings.

1.6 Research Delineations

This research project investigated and developed a cost-effective test setup for EMC testing specifically tailored for F'SATI CubeSats. The project focused on implementing RE testing methodologies suitable for the size and design constraints of CubeSats.

The delineations of this research were as follows:

- **Scope:** The project was limited to the development of a test setup for EMC pre-compliance testing, specifically RE, for CubeSats developed by F'SATI.

[2] Although an anechoic chamber is considered the gold standard for full EMC compliance testing, access to such a facility was not readily available for this research. Instead, a reverberation chamber was selected as a suitable comparison for pre-compliance testing. While anechoic chambers provide a fully controlled free-space environment, reverberation chambers introduce additional RE modes, making them a viable and practical alternative within the scope of this study.

- **Functionality:** The test setup focused on pre-compliance testing, providing data to identify potential EMC issues during the design phase.
- **Complexity:** The research focused on a cost-effective solution and did not explore highly specialised or expensive equipment.
- **Integration:** While the project aimed to develop a testing methodology, integration of this methodology within F'SATI's CubeSat design process was outside the scope of this research.
- **System-level testing:** While the importance of system-level testing was acknowledged, this project concentrated on the development of a test setup for subsystem-level testing.

This delineations clarifies that the project's main deliverable was a cost-effective EMC test setup designed for F'SATI's CubeSat subsystems, focusing on RE pre-compliance testing during the design phase.

1.7 Thesis Layout

This thesis is structured to provide a comprehensive overview of the development and implementation of a radiated emissions test setup for CubeSats. The document is divided into several chapters, each addressing specific aspects of the research and development process. Below is a summary of each chapter's content:

1.7.1 Chapter 1: Introduction

The introductory chapter establishes the background and context of the study. It discusses the significance of CubeSats in modern space missions, the importance of EMC in ensuring the functionality of these satellites, and the challenges faced in EMC pre-compliance testing. The research problem, objectives, and questions are clearly outlined to set the stage for the subsequent chapters.

1.7.2 Chapter 2: Literature Review

A review of existing literature related to EMC, focusing on the fundamentals, importance, and regulations surrounding EMC. Various EMC pre-compliance testing and measurement techniques are examined, with a particular emphasis on radiated emissions. Additionally, the use of transverse electromagnetic (TEM) cells in EMC pre-compliance testing is explored, highlighting previous research and methodologies.

1.7.3 Chapter 3: TEM Cell Design

The TEM cell design chapter outlines the design, simulation, and fabrication processes involved in creating the TEM cell. Design considerations, including the TEM cell's dimensions, supports, septum, and walls, are detailed. The simulation results, optimization procedures, and the steps taken to manufacture and assemble the TEM cell are discussed, along with the practical implementation of the test setup.

1.7.4 Chapter 4: Manufacturing

This chapter describes in short the manufacturing process, what software was used and the challenges that came with the manufacturing process.

1.7.5 Chapter 5: Verifications Testing

Verifications testing is for focusing on the evaluation of the TEM cell. The equipment used, measurement procedures followed, and the outcomes of various tests conducted are described. The performance of the TEM cell in accurately measuring radiated emissions, ensuring the EMC of CubeSat components, is analyzed.

1.7.6 Chapter 6: Discussion

This chapter interprets the results obtained, emphasizing their implications for CubeSat subsystems. The increased usable test area provided by the developed TEM cell and additional considerations for improving EMC pre-compliance testing are discussed. Recommendations for future research and potential improvements to the TEM cell design are also provided.

1.7.7 Chapter 7: Conclusion

A summary of the key findings of the research, highlighting the successful development and implementation of a cost-effective TEM cell for EMC pre-compliance testing of CubeSats. The importance of early-stage EMC pre-compliance testing and the potential for academic institutions to contribute to EMC compliance in the space industry are underscored.

1.7.8 Appendices

The appendices section includes additional information supporting the research, such as project budget, time management, manufacturing drawings, and design notes. These appendices provide detailed insights into the project's execution and technical specifics.

Chapter 2

Literature Study

2.1 EMC

2.1.1 EMC Fundamentals

To achieve EMC, understanding its three fundamental elements is essential: source, coupling path, and victim. The source generates unwanted electromagnetic noise, which can be artificially generated or controlled during EMC tests. The coupling path is the means by which the noise from the source reaches the victim, which is the noise receptor (Paul 2006). Figure 2.1 below provides examples of sources, victims, and coupling paths.

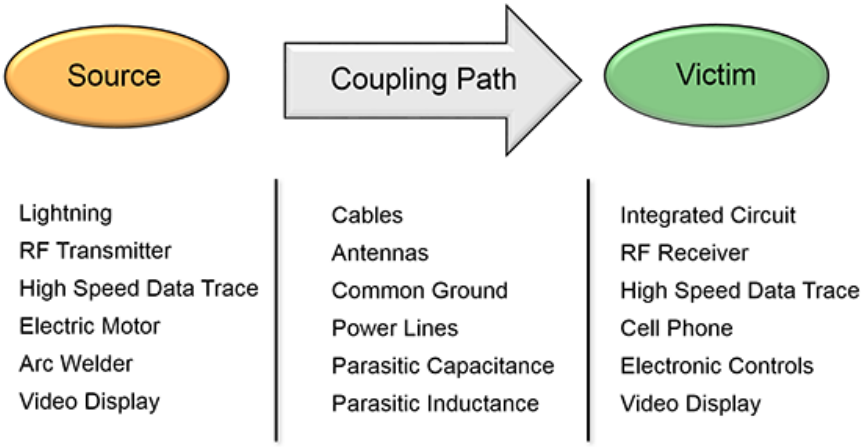

Figure 2.1: Three EMC Elements (EMC Learn 2020)

According to *Introduction to electromagnetic compatibility*, EMC issues can generally be addressed by identifying any two of the three contributing elements and removing at least one, thereby achieving EMC compliance. A thorough understanding of these foundational principles is essential for grasping the significance and regulatory requirements associated with EMC. In this project, the CubeSat subsystems are identified as sources of RE, with neighbouring subsystems considered as potential victims. Thus, analysis criteria can be fulfilled by measuring the RE levels of each subsystem and designing both the system and subsystems to mitigate interference accordingly.

2.1.2 EMC Importance & Regulations

EMC issues can cause various unexpected effects on electronic devices. Several documented examples include a light bulb that interferes with a television (Media 2020a), an explosion in a passenger jet that causes the loss of 230 lives, turbine control valves of a nuclear power plant that spontaneously close (EMC Learn 2020), and overhead trains that interfere with the readings of the Large Hadron Collider (Media 2020b). These are just a few of many instances of EMC problems that range from minor inconveniences to catastrophic failures. This underscores the importance of rigorous EMC testing for all electronic devices.

To further emphasize its significance, several regulatory bodies at both the international and national levels have established standards to address EMC issues:

1. International Electrotechnical Commission (IEC)
2. Comité International Spécial des Perturbations Radioélectriques (CISPR)
3. International Organization for Standardization (ISO)
4. Comité Européen de Normalisation (CEN) (Europe)
5. Federal Communications Commission (FCC) (USA)

Furthermore, to address the specific EMC challenges in space engineering, the European Cooperation for Space Standardization (ECSS) has developed standards such as the space engineering EMC handbook ECSS E-HB-20-07A (European Space Agency 2012a) and the space engineering EMC standard ECSS E-ST-20-07C Rev.1 (European Space Agency 2012b). These documents primarily focus on spacecraft design considerations for space environments, outlining compliance requirements for fully operational satellites.

However, this project focuses on pre-compliance testing for CubeSat subsystems rather than full spacecraft qualification. Pre-compliance testing aims to identify and mitigate EMC issues early in development, reducing the risk of costly failures during final compliance testing. Unlike the ECSS standards, which primarily address mission-ready space systems, the IEC and CISPR regulations provide well-established methodologies for laboratory-based EMC testing applicable to a broad range of electronic devices, including CubeSat components.

Therefore, while ECSS guidelines provide valuable reference material for CubeSat developers, the pre-compliance test setup developed in this project aligns more closely with the widely accepted regulatory frameworks of IEC and CISPR, ensuring that testing procedures remain consistent with industry standards used for early-stage EMC validation.

2.1.3 EMC Testing & Measurements

In EMC the test setup is determined by the type of measurement, and whether it involves immunity, susceptibility, radiated emissions, conducted emissions, magnetic fields, electric fields, or radio frequency signals. Figure 2.2 illustrates the main types of EMC tests.

During these EMC tests the measurements must fall within the allowable range specified by the relevant standards or internal testing requirements.

When performing preliminary in-house tests for EMC compliance it is called pre-compliance testing. It is refereed to in this way because the equipment does not usually have the necessary accuracy to predict full compliance. However, pre-compliance testing plays a crucial role in the EMC compliance process by identifying potential issues early, thus saving time and costs. This phase often involves the use of TEM cells, near-field probes, and spectrum analysers.

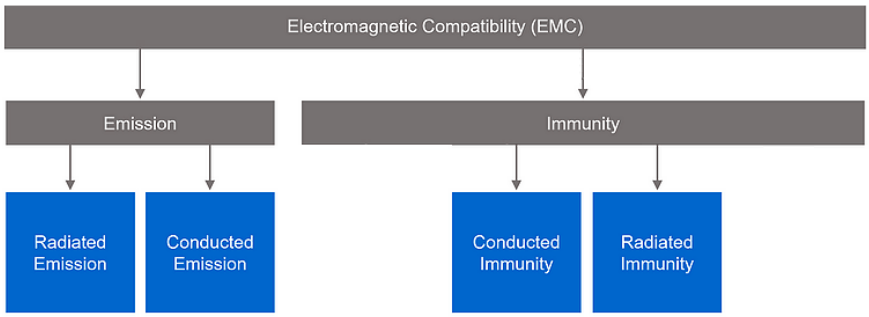

Figure 2.2: EMC emission and immunity diagram (Academy of EMC 2020)

This project will be focusing on RE testing and how to develop a cost effective method to produce equipment that can do so. The types of equipment generally used to measure the EMC components as in figure 2.2 are further discussed and compared in chapter 2.1.5 below.

2.1.4 Radiated Emissions

The emissions of electronic equipment or systems, known as RE, have the potential to interfere with the normal operation of other electronic equipment or systems. Accurate determination of the characteristics of these emissions is essential for ensuring EMC (M. Crawford and Workman 1979). The ECSS specifies that a given unit of spacecraft requirements can be specified over the entire 30 MHz - 18 GHz range or only the relevant receive bands (European Space Agency 2012a). For CubeSats, which typically have mission-specific equipment, testing will be carried out on the relevant bands depending on the equipment used.

2.1.5 EMC Testing Equipment

As of 2024, several established methods are available for testing EMC, primarily for compliance verification. These methods, however, are generally costly and require significant space and resources to implement independently. Some of the key testing chambers include the following:

- **Anechoic Chambers**
- **Reverberation Chambers**
- **Semi-Anechoic Chambers (SACs)**
- **GTEM Cells**
- **TEM Cells**

Depending on the specific EMC testing required, one of these chambers will be used, as described in the following sections. While these facilities are typically large and designed for substantial devices, this project focuses on CubeSats, requiring smaller, scaled-down versions. This will provide a more realistic view regarding the use case of students on campus and compared to other methods more like TEM cells due to the compact nature.

Anechoic Chambers

Anechoic chambers are designed to absorb electromagnetic waves, providing a controlled environment free from external interference. They are commonly used for emissions and immunity testing, simulating open-air conditions with high accuracy. These chambers are advantageous for their ability to offer a highly controlled testing environment and to closely replicate free-space conditions, which enhances the precision of emissions and immunity tests across a wide range of frequencies. However, anechoic chambers are often costly to construct and maintain, requiring significant space and specialized materials, which may limit their feasibility for smaller-scale applications.

In figure 2.3 below, one can see a fully anechoic 3-meter EMC test chamber, which was installed new in 2012 and professionally dismantled in 2018. This chamber is designed to perform ANSI C63.4/CISPR 16-1-4 and IEC 61000-4-3 fully compliant radiated immunity measurements and is also used for pre-compliant radiated emissions measurements. Full NSA data is available, showing an accuracy of ±6dB. The frequency ranges for this chamber are 26 MHz to 6 GHz for radiated immunity and 30 MHz to 18 GHz for radiated emission (TheEMCShop 2024b).

Figure 2.3: 3 Meter Anechoic Chamber(TheEMCShop 2024b)

Reverberation Chambers

Reverberation chambers create a highly reflective environment that produces a statistically uniform electromagnetic field, making them suitable for immunity testing, particularly under high field strengths. They are highly efficient for testing immunity across multiple frequencies and are often a cost-effective choice for large devices, as their reflective design distributes electromagnetic fields evenly within the chamber. Nonetheless, reverberation chambers are generally unsuitable for precise emissions testing due to the complexity of isolating emissions within a highly reflective space. Additionally, their high field strengths can present challenges when testing sensitive electronics.

In the figure 2.4 below, one can see a Teseq RC Chamber 2XS Reverberation Chamber, available for shipping to North America and Western European countries. This chamber is designed for emission and immunity testing, complying with standards such as IEC 61000-4-21:Ed.2, MIL461F, and RTCA DO160F. The chamber dimensions are 1.5m x 0.8m x 1.0m, with a working volume size of 0.5m x 0.3m x 0.5m. It features a stirrer to change the electromagnetic field inside the chamber, behaving like a multi-mode resonator. The frequency range is 0.8 to 18 GHz, with typical shielding effectiveness of $\geq$ 80 dB. The chamber walls are made of aluminium, and it weighs approximately 96 kg (TheEMCShop

2024a).

Figure 2.4: Reverberation Chamber(TheEMCShop 2024a)

Semi-Anechoic Chambers (SACs)

Semi-anechoic chambers feature absorbing materials on the walls while retaining a conductive ground plane, allowing them to simulate open-area test sites in a controlled indoor setting. They are versatile for both emissions and immunity testing, as they replicate real-world open-area conditions while minimizing external noise. Semi-anechoic chambers are practical for testing mid-sized to large devices. However, they still require substantial space and involve high operational costs. Additionally, they may not achieve the same level of isolation from environmental interference as fully anechoic chambers, which can impact the accuracy of certain sensitive tests.

Figure 2.5 below, shows an image of a semi-anechoic 3-meter EMC test chamber. This chamber is designed to perform ANSI C63.4/CISPR 16-1-4 and IEC 61000-4-3 fully compliant radiated immunity measurements and is also used for pre-compliant radiated emissions measurements. Full NSA data is available, showing an accuracy of ±6dB. The frequency ranges for this chamber are 26 MHz to 6 GHz for radiated immunity and 30 MHz to 18 GHz for radiated emission.

Figure 2.5: Semi-Anechoic Chamber(TheEMCShop 2024c)

Gigaherz Transverse-Electromagnetic (Mode) (GTEM) Cells

GTEM cells are compact, closed structures that can operate at frequencies up to several GHz, providing a reliable setup for emissions and immunity testing of compact electronic devices. GTEM cells are advantageous in that they occupy less space than traditional chambers, making them ideal for smaller-scale testing environments, and they provide an efficient pre-compliance testing option at high frequencies. However, they have limited applicability for testing larger devices and can sometimes lack the precision of larger anechoic chambers for emissions measurements due to field uniformity constraints at the chamber edges.

In the image 2.6 below, the TBGTC1 is shown as an open GTEM cell specifically designed for EMC pre-compliance testing. This compact testing device, developed by Tekbox, provides an alternative to traditional anechoic chambers for radiated emissions and immunity testing, especially useful in early design phases. Unlike traditional TEM cells, GTEM cells extend the operational frequency to several GHz, supporting a range of 0.009 MHz to 6 GHz. The cell is compact, with external dimensions of 1452 x 780 x 520 mm and a weight of 13 kg, making it practical for lab environments. It accommodates devices under test (DUT) with maximum dimensions of 200 x 200 x 150 mm. The TBGTC1 operates as a 50-ohm stripline terminated at the end, allowing it to detect emissions from the DUT or to radiate controlled RF fields for immunity testing. The device's open design enables easy placement of the DUT but may pick up background RF noise, which can be mitigated through calibration or an optional shielded tent. The GTEM cell has a nominal impedance of 50 ohms, a VSWR of 1:1.3 (typical), and allows RF input power up to 600 W for testing field strengths. For accurate pre-compliance results, it adheres to IEC 61000-4-2 standards and provides uniform field distribution up to 3 GHz (Eadie 2019b).

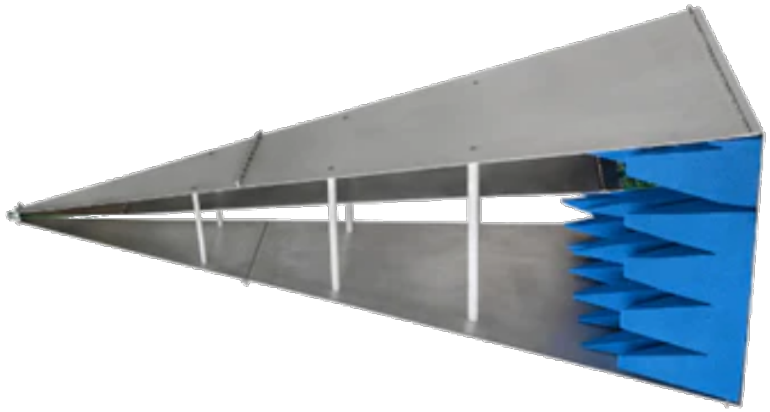

Figure 2.6: GTEM Cell(Eadie 2019a)

TEM Cells

TEM (Transverse Electromagnetic) cells produce a standardized electromagnetic field, making them well-suited for emissions and immunity testing of small devices at lower frequencies. TEM cells are advantageous in their compact size, ease of use, and affordability compared to larger chambers. However, they are limited to low-frequency testing and may not offer the same level of control over high-frequency emissions, which could restrict their use in certain high-performance applications.

In the image below, the Tekbox TBTC series open TEM cells are designed for EMC pre-compliance testing, offering a cost-effective alternative to large anechoic chambers. These cells, specifically models TBTC0, TBTC1, TBTC2, and TBTC3, cover a frequency range up to 2 GHz and can identify radiated emissions and immunity issues within electronic devices. Each TEM cell consists of a central conductive strip, or septum, within a grounded enclosure, creating a 50-ohm transmission line for testing.These open TEM cells provide practical benefits due to their compact design and affordable setup, allowing smaller enterprises to conduct preliminary EMC testing in-house. The cells operate by picking up radiated noise from the device under test (DUT) using the septum, which acts similarly to a broadband antenna, and routing the signal to a connected spectrum analyser. For immunity testing, an RF amplifier drives the septum to radiate a controlled RF field into the DUT, enabling evaluation of susceptibility to interference. Tekbox TEM cells offer enhancements in frequency response due to a unique design that suppresses higher-order wave modes, resulting in improved performance compared to traditional TEM cells. Each unit includes a 50-ohm termination and a DC block to protect measurement equipment from potential over voltage. While the cells do not provide full shielding from ambient RF noise, external noise can typically be accounted for by performing a baseline measurement prior to testing the DUT. This setup is ideal for iterative design adjustments, allowing engineers to assess the impact of modifications on EMC performance and avoid costly compliance test failures (Eadie 2019a).

Figure 2.7: TEM Cell(Eadie 2019a)

Each of these facilities serves specific purposes within EMC testing, selected based on the emission, immunity, and environmental simulation requirements of the device under test. The pros and cons of each chamber type guide their suitability for different devices and testing environments. Considering for space, cost, and frequency range the table 2.1 below was made with estimated values.

Table 2.1: Comparison of EMC Testing Facilities

Testing Facility	**Size (m)**	**RE Test Range**	**Cost**
Anechoic Chamber	3.0 x 3.0 x 3.0	0.03 - 18 GHz	R 10 M
Reverberation Chamber	1.5 x 0.8 x 1.0	0.8 - 18 GHz	R2 M
GTEM Cell	1.4 x 0.78 x 0.52	9e-6 - 6 GHz	R 100 000
TEM Cell	0.45 × 0.25 × 0.16	0.001 - 3 GHz	R 30 000

Using the equipment above to conduct pre-compliance testing, potential issues can be identified early, allowing necessary design modifications to improve the likelihood of reaching compliance. This approach reduces the number of formal compliance tests needed, thereby lowering the overall project cost. As shown in Table 2.1, TEM and GTEM cells are the most efficient solutions for RE testing in terms of cost and space. These cells are suitable for pre-compliance testing as long as the required test frequencies remain within the operational range of the TEM and GTEM cells(**RQ5 p.12**, **RQ6 p.12**, **RQ7 p.12**, **RQ12 p.12**).

While chambers provide better shielding from environmental interference, which is beneficial for high-accuracy measurements, pre-compliance testing, to a certain extend, can typically prioritizes cost-effectiveness over shielding. In many cases, this trade-off is acceptable, particularly when EMI-quiet rooms are available, as is common in electrical engineering buildings on university campuses. Furthermore, TEM cells have been utilized in certain compliance certification tests for RE and Radiated Susceptibility (RS) according to IEC 61000-4-3 standards, which underscores their versatility and effectiveness in pre-compliance testing. As noted by Sandeep M. Satav 2008, the TEM cell is recognized as a valuable and cost-effective tool for internal pre-compliance testing. With these comparisons the TEM and GTEM cells stand out as the most cost effective and spatially efficient means EMC tests on Cubestats.

2.1.6 EMC Testing Using TEM and GTEM Cells

TEM or GTEM Cells

Given their cost-effectiveness compared to anechoic, semi-anechoic, and reverberation chambers, both TEM and GTEM cells present ideal solutions for educational settings. As outlined in "Do-it-Yourself Fabrication of an Open TEM Cell for EMC Pre-compliance", students can construct their own TEM cells using affordable materials and standard equipment typically available on campus. The measurement process involves common laboratory tools, such as signal generators and spectrum analysers, as described in subsection below. The primary difference between TEM and GTEM cells is their operational frequency range. Since "Do-it-Yourself Fabrication of an Open TEM Cell for EMC Pre-compliance" focuses on TEM cells, they are the most suitable choice for this project, because it can facilitate an informed starting point. Additionally, the head of F'SATI has specified a testing range from DC to 2 GHz, which aligns well with the capabilities of a TEM cell. That is, the higher frequency ranged proved by a GTEM cell is not required.

Focusing on the development of a TEM cell not only provides a cost-effective method for EMC pre-compliance testing but also offers students valuable hands-on experience in understanding RE through the cell construction process. With the information available in "Do-it-Yourself Fabrication of an Open TEM Cell for EMC Pre-compliance" as a staring point, this thesis will develop as a practical guide for students. This will enhance their EMC knowledge by enabling them to design and construct a TEM cell tailored to specific frequency testing needs and device sizes. This approach benefits future students by providing them with both the theoretical and practical framework to conduct EMC testing independently and cost-effectively (**RQ4 p.11**).

Other Equipment Required

Essential equipment includes a spectrum analyser or oscilloscope, coaxial cables with N-type connectors, and E and H-field probes. The TEM cell provides an overall assessment of RE, identifying whether any CubeSat subsystem emits radiation at levels that could interfere with surrounding subsystems. However, if a problematic frequency range is detected, additional tools are needed to pinpoint the exact source of the emissions.

In such cases, E and H-field probes serve as a valuable addition to the test setup, allowing for localized measurements that help identify which specific component within the subsystem is responsible for the emissions. This facilitates targeted redesigns to mitigate interference while ensuring overall EMC pre-compliance. The TEM cell helps detect problematic frequencies at a higher level, while E and H-field probes enable more detailed fault tracing at the Printed Circuit Board (PCB) level (**RQ2 p.11**). Although maintaining adequate separation between subsystems can help reduce interference, the compact nature of CubeSats often necessitates precise PCB analysis to prevent unforeseen issues before final testing and launch.

2.2 Developing TEM Cells

The transverse electromagnetic mode, abbreviated TEM, has a specific field radiation pattern perpendicular to the propagation direction. The TEM cell is constructed as a rectangular coaxial transmission line with tapered sides, enabling the TEM mode over a certain frequency range that depends on the dimensions and materials of the cell. Although this range typically extends from DC to a few hundred MHz, it can be designed to cover the entire frequency range up to at least 1 GHz (Bentz 1996).

Figure 2.8 below shows an example of an open tri-plate cell TEM.

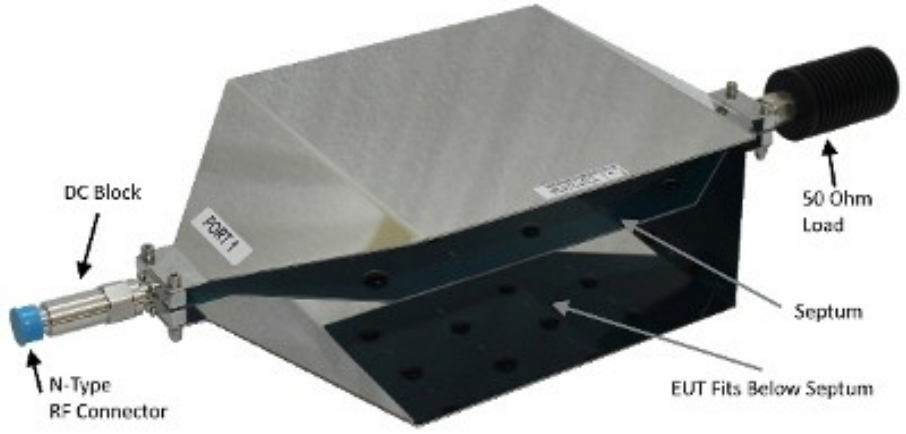

Figure 2.8: Tri-plate open TEM (Eadie 2019c)

When using a TEM cell for measurements, a few things should be taken into account.

2.2.1 Ambient Noise

The use of an open TEM cell often results in the observation of signals of ambient noise. To mitigate this, tests can be conducted in a EMI quiet room or a shielding bag (figure 2.9 can be used for the TEM cell. Another effective method is to adjust measuring techniques by reducing the analyser span, focussing on one peak, and decreasing the Resolution Bandwidth (RBW) to 10 kHz or lower. This reveals emissions that may have been obscured by higher ambient signals. (Eadie 2019c)

Figure 2.9: Shielding Bag

2.2.2 Noise Floor

According to Eadie from EMC Fast Pass, emission from Device Under Test (DUT) in TEM cells may sometimes be below the noise floor displayed on a spectrum analyser, presenting a common issue (ibid.). To enhance the detection of these emissions, a preamplifier with a gain of around 20-40 dB can be inserted between the TEM cell and the spectrum analyser. However, this introduces the risk of overloading the analyser's input stage, potentially causing distortion, inaccurate readings, or even permanent damage to its sensitive front-end components if the signal exceeds its maximum input power rating.

2.2.3 Characteristic Impedance

Characteristic impedance is a fundamental parameter in electromagnetic transmission lines, including TEM cells. It describes the ratio of voltage and current waves propagating along the line. In TEM cells, characteristic impedance is crucial because a mismatch between the line's characteristic impedance and the load can lead to significant reflections at the measurement port, affecting measurement accuracy.

The characteristic impedance of a TEM cell is typically calculated based on the cell's dimensions and material properties. It should be designed to match the load impedance for optimal power transfer and minimal reflection. In most cases, including this study, a characteristic impedance of 50 Ω is targeted.

The characteristic impedance of the transmission line is determined, according to M. L. Crawford, by fixed dimensions of the line's cross-section and an unknown fringing capaci-

tance per unit length C'_f. It can be calculated using the equation:

$$Z_0 = \frac{94.15}{(\epsilon_r)^{\frac{1}{2}}[\frac{w}{b(1-t/b)} + \frac{C'_f}{0.0885\epsilon_r}]}$$

Where ϵ_r is the dielectric constant of the medium between the conductors, w, b and t are dimensions displayed in figure 2.10 and C'_f is the fringing capacitance (pF/cm).

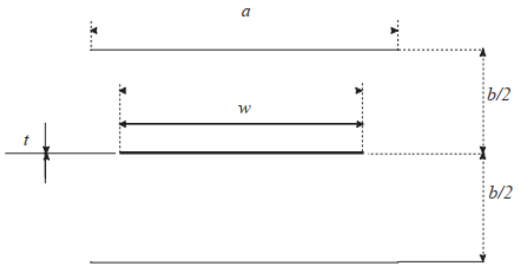

Figure 2.10: TEM cross-sections (Malaric and Bartolic 0203)

2.2.4 Dimensions

The dimensions of a TEM cell are governed mainly by its characteristic impedance and the usable frequency range. The characteristic line impedance of the TEM cell is calculated using a formula that takes into account the relative dielectric constant of the medium within the cell, the width and thickness of the septum, the distance between the septum and the upper wall, and the fringing capacitance per unit length. Using these formulas as design guidelines, the dimensions of the cell—such as height, width, length, and tapering—can be calculated (Sandeep M. Satav 2008). While tapering does not have a specific formula, its calculation follows logically from the other equations, as explained in more detail in section 3.2.4

2.2.5 Radiated Emissions Test Setup

One of the notable advantages of a TEM cell is its simplicity in setup. The test setup involves connecting one port to a termination resistor (dummy load) while the other port is connected to a spectrum analyser through a DC block (if desired). The DUT is then placed between the septum and the outer conductor, allowing measurements to be taken (Tekbox Digital Solutions 2020). Figure 2.11 depicts the schematic of the test setup.

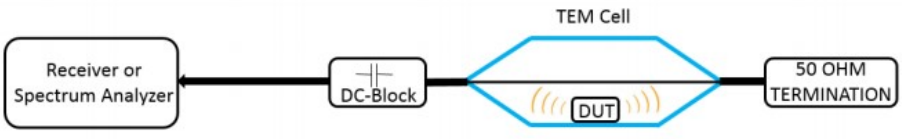

Figure 2.11: Radiated Emissions TEM Cell Setup (Tekbox Digital Solutions 2020)

After the setup is completed, the DUT is operated as normal to measure the RE projected from it.

2.2.6 Modelling & Simulating

FEKO, an EM simulation software, was utilized to model the calculated dimensions of the TEM cell design and simulate its EM behaviour. The simulation results were assessed, focusing on the reflection coefficient at the measurement port, to verify that reflections were sufficiently low to ensure accurate measurements. This criterion was met as the reflection coefficient was determined to be below -10dB[1]. . The evaluation confirmed whether the design met the desired performance specifications and was deemed suitable for the manufacturing phase.

[1]Further discussion on -10dB value in Chapter 3.1.

Chapter 3

TEM Cell Design

3.1 TEM Cell Design and Simulation

Design Procedure

The procedure for designing the TEM cell began with understanding and categorizing its design parameters by understanding the methodology in "Do-it-Yourself Fabrication of an Open TEM Cell for EMC Pre-compliance" and building from there. After the methodology was better understood the subsequent focus was identifying the inherent physical attributes of the cell that could not be altered. These attributes included factors such as the specific equipment to be tested, the analytical instruments used for data acquisition, and the method of connecting these analytical instruments to the cell. By pre-selecting these key physical parameters, they could be incorporated into the design process as constraints.

Once the primary physical constraints of the cell were determined, the next step involved examining the EM design considerations of the cell and how they are effected by the physical design. These considerations were compartmentalized into the different types of transmission line disciplines that make up the TEM cell, such as the Coax To Stripline (CTSL) transition and the STWS transition. This enabled simpler simulation as the individual components have less criteria to evaluate. The individual components were then assembled and simulated as a unified unit that make up the full TEM cell (**RQ9 p.12**).

Literature

As previously mentioned, to establish the foundation for the design process of the TEM cell, the article titled "Do-it-Yourself Fabrication of an Open TEM Cell for EMC Pre-compliance" (Sandeep M. Satav 2008) was used as a comprehensive reference. Furthermore, a review of the contemporary literature was carried out, including " "Design of a TEM cell using both multi-step and piecewise linear tapering"" (Arezoomand, Kalantari Meybodi, and Noori 2016), " "Design and Characteristic Calibration of TEM Cell for IC Radiation EMC Test"" (Ho et al. 2019), and " "3D-Printed Low-Cost and Lightweight TEM Cell"" (Al Takach et al. 2018), to incorporate high-quality design considerations. Although not all inputs were directly applied to this specific project, they significantly improved the understanding of various design methodologies and criteria. Researchers undertaking similar projects may find value in exploring these resources to complement their own investigations and replicate successful outcomes.

Software

To accelerate the mathematical iterative process MATLAB (MathWorks 2021) was used for the necessary calculations and graphing. The obtained dimensional values were then utilized to construct a comprehensive model using Altair: Feko (Altair University 2021), a powerful software tool for high-frequency electromagnetic simulations. These simulations facilitated meticulous evaluation of EM characteristics, ensuring compliance with the desired manufacturing performance requirements. It also enabled the export of data for further analysis and graphing in MATLAB.

Subsequently, Autodesk: Inventor (Autodesk 2021) helped to create manufacturing drawings once the simulation output was deemed satisfactory. Following this systematic approach, the design process for the TEM cell successfully integrated both theoretical calculations and practical considerations, resulting in an optimized design.

Please see below a flow chart that outline the design methodology.

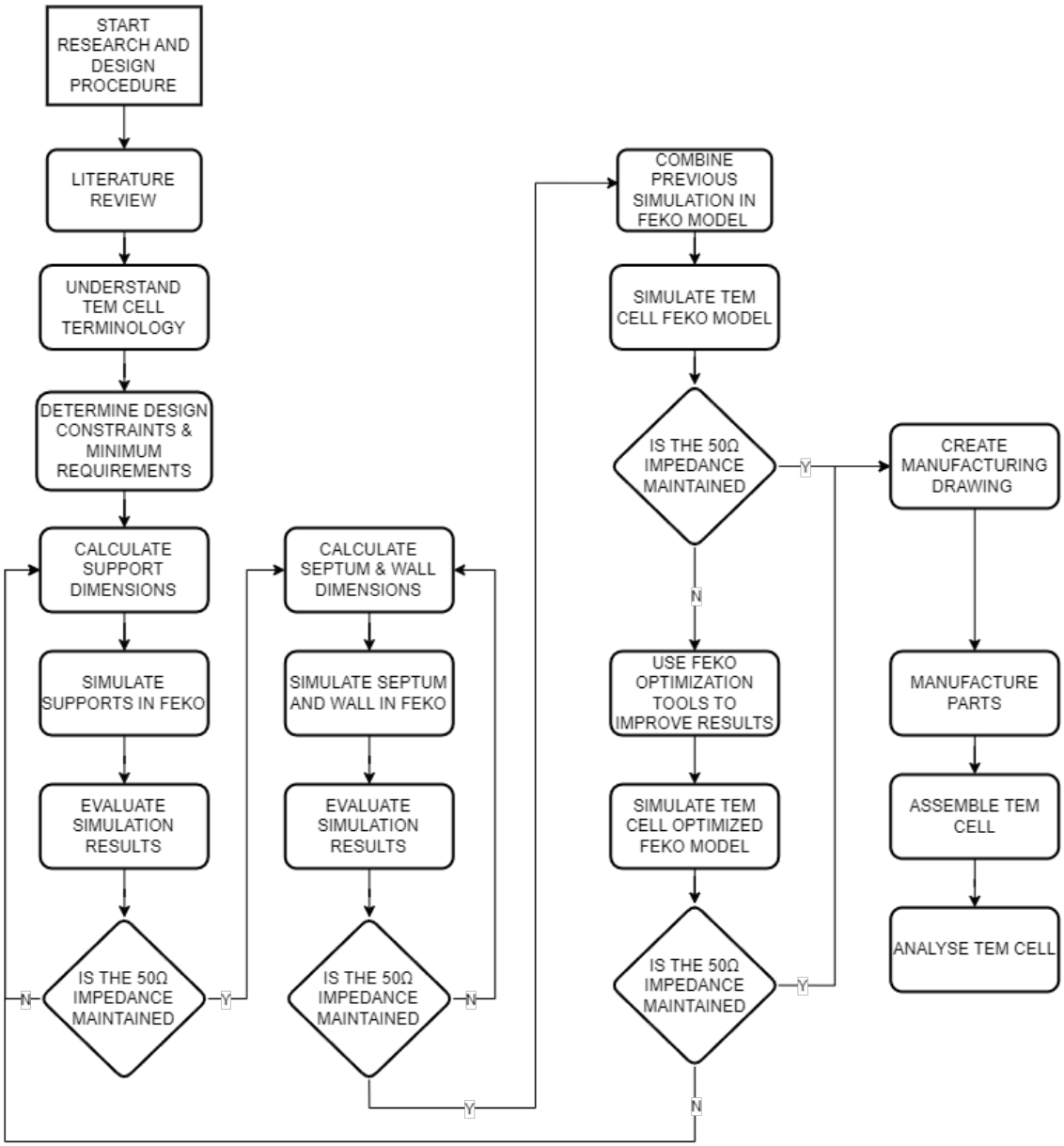

Figure 3.1: Research Plan

3.2 TEM Cell Design Considerations

The design of a TEM cell encompasses various critical aspects, such as the physical dimensions of the DUT, the configuration of the connection point of the analyser, and the smooth transition from the connection point to the remaining sections of the TEM cell. It is crucial to address and engineer these elements meticulously to ensure accurate preservation of a 50 Ω impedance throughout the entire TEM cell, spanning the frequency spectrum of DC to 2GHz.

3.2.1 TEM Terminology

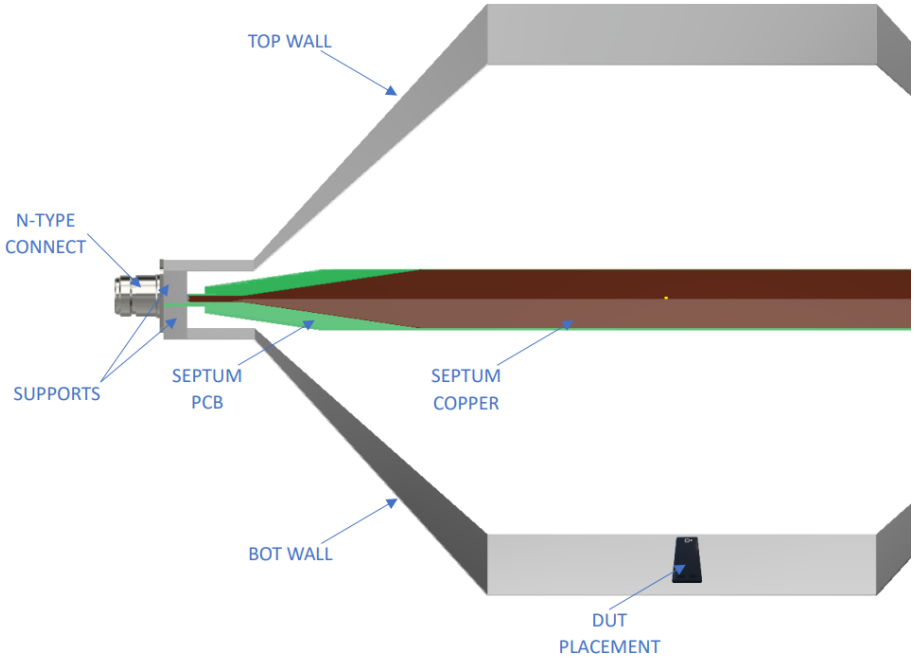

Figure 3.2: Terminology

To begin the design and review of a TEM cell involved defining and understanding the various components that make up the cell. Clear definitions of these components are essential to analysis in design to assure good communication of the design and consistent analysis.

Wall

The upper and lower walls of the TEM cell are grounded planes made of laser cut and bent aluminium. These walls serve the critical function of maintaining a constant 50 Ω impedance throughout the length of the TEM cell. This impedance matching is vital to ensure accurate and reliable measurements.

DUT

The DUT refers to the components being evaluated using the TEM cell. In this project, the primary focus of the DUT is the RE of the components used in CubeSats. Accurate measurement of the DUT electrical characteristics is crucial to assess the performance and functionality of these components in a CubeSat environment.

Connector

The selection of the connector for the TEM cell depends on the specific equipment used to measure the characteristics of DUT. Two connectors are required on each side of the TEM cell: one to connect to the equipment used to analyse the DUT, and another for the dummy load. Connectors should be carefully chosen to minimize losses and maintain signal integrity throughout the measurement process.

Septum

The septum, is the central component of the TEM cell. It plays the crucial role of measuring RE of DUT. In other design cases, when testing for susceptibility it also the means through which the DUT is radiated with EM radiation in order to test for RS.

Supports

The TEM cell is held together by machined stainless steel supports. Four supports are utilised, two located on each side of the TEM cell. These supports provide structural stability and alignment for the entire cell assembly. Their precise machining ensures proper positioning of the walls, septum, and connectors, maintaining the integrity of the TEM cell design.

3.2.2 Design Constraints

The size of the TEM cell is influenced by the dimensions of the DUT. To establish the minimum dimensions, engineers from F'SATI were consulted. They indicated that most of the subsystems, excluding special mission specific devices, do not exceed the size of the battery system. Therefore, the optimus-40 battery from Space (Figure 3.3) was selected as a reference, given its widespread usage in CubeSat applications.

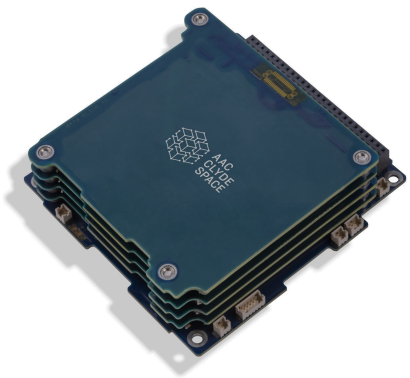

Figure 3.3: OPTIMUS-40 (Space 2023)

According to the data sheet, the optimus-40 battery measures 100x100x27.30mm (WxDxH). To allow technicians ample space to manoeuvrer the device during testing, the minimum width and depth of the TEM cell were determined to be 150 mm. Furthermore, regarding the height between the bottom wall and the septum. According to "Generation of Standard EM Fields Using TEM Transmission Cells", one third of the height between the bottom wall and the septum can be occupied by the DUT during testing. This one third factor is considered the maximum that the impedance loading effects from the DUT do

not adversely affect the EM field perturbation of the TEM cell. With the height of the optimus-40 being 27.3 mm, the height constraint from the bottom wall to the septum set to be a minimum of 90 mm. This provides a good initial design criteria for the physical design of the cell and further developed could commence from this point. In figure 3.4 these design constraints are lustrated.

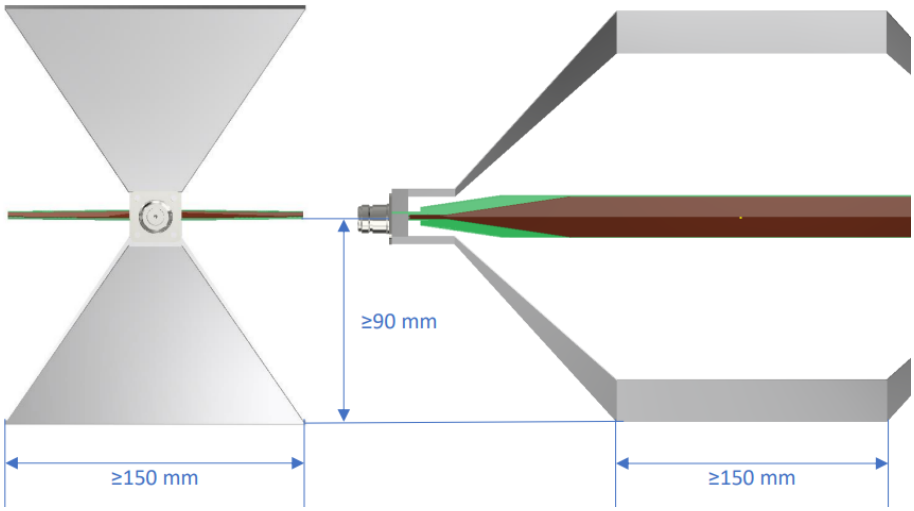

Figure 3.4: Minimum Allowable Dimensions

3.2.3 Supports

Starting with physical constraints, the supports are used to connect the individual parts of the TEM cell together and therefore require mounting holes for each respective component. An illustration of the a conceptual design with these mounting holes can be seen in figure 3.5.

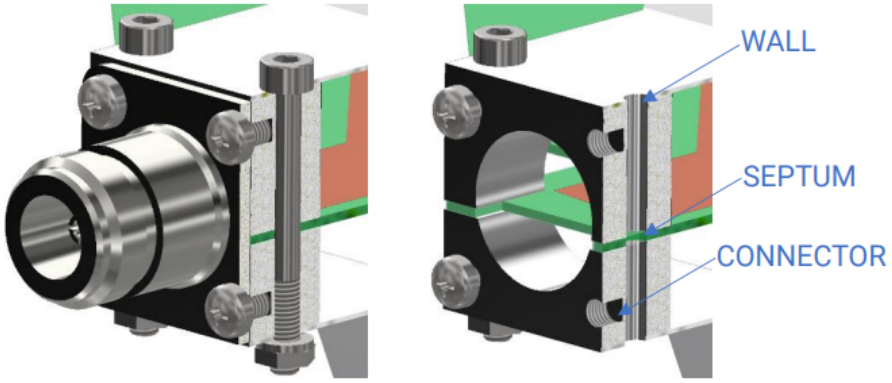

Figure 3.5: Mounting holes

The size of the supports are determined by the selected connector. For this project, N-type connectors were used at both ends of the TEM cell: one for the analyser and the other for a 50 Ω dummy load. According to the supplier's specifications, the connector size is 25.4 x 25.4 mm (fig 3.8), which was the starting size of the TEM cell supports. At this point in the design the two halves of the a support is identical, except for the slight offset required to connect the pin of the N-type connector to the septum. The offset dimension corresponds to the radius of the N-type connector pin, as illustrated in figure 3.6 below. The pin is 3mm, the offset is therefore 1.5mm.

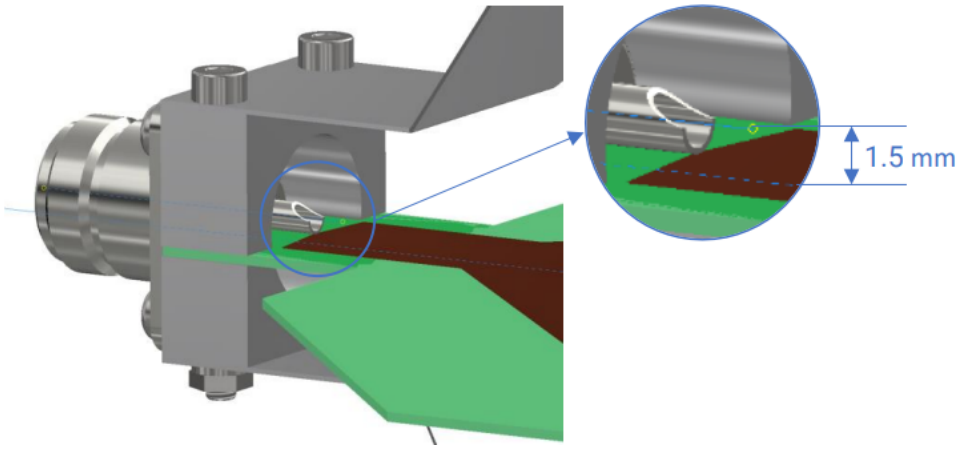

Figure 3.6: Support Offsets

With the physical constraints of the support design established, the appropriate radius of the supports needed to be determined to maintain a 50Ω impedance until the transition from coaxial to stripline was made.

There is limited information available on open TEM cells, and even less on the design of their connection points. This oversight is significant because the connection point is where the coaxial-to-stripline transition occurs.

Without proper investigation, this transition could have become a point of impedance mismatch. This needed to be avoided as far as possible, since a mismatch what cause reflection that would make the readings inaccurate. Therefore, the design of the TEM cell considers the connection point as a crucial factor in both calculation and analysis. To evaluate the impact of the connector, the type of connector was selected, and its physical and EM attributes were analysed. In this project, this was done by replicating the scenario as accurately as possible in FEKO and running simulations as described below. This approach allows the design of the TEM cell to be adjusted to accommodate the connector in a manner consistent with coaxial design practices.

The supports of the TEM cell serve as mounting points for the connector, as illustrated in figure 3.5. They also provide the foundation for assembling the remaining components, including the septum and walls. The support therefore ended to be made from a strong conductive material due to its smaller size in comparison to the rest of the TEM cell it needs to support. Therefore the supports consists of two laser cut stainless steel parts with a calculated diameter determined by equation 3.1.

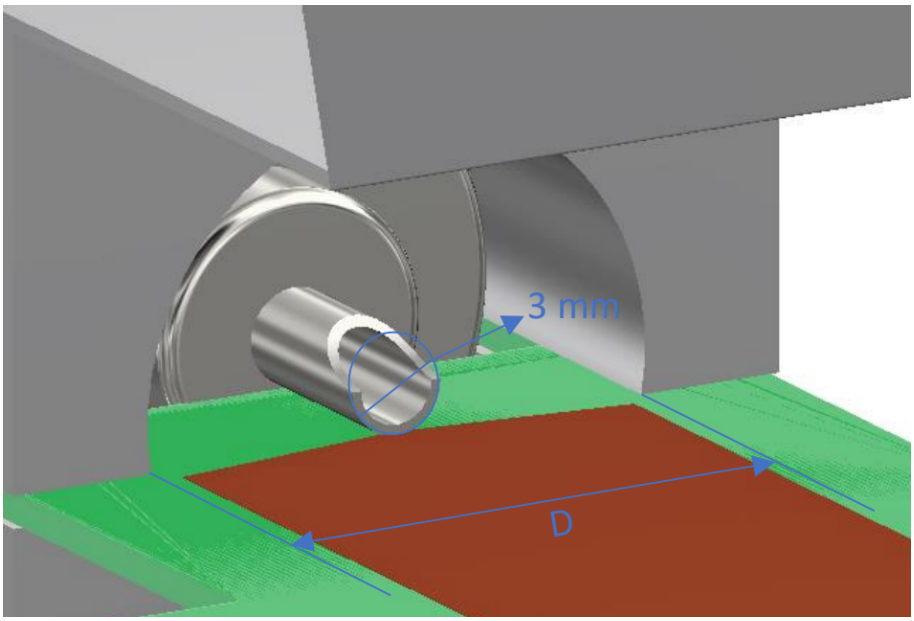

Figure 3.7: Connection Length

The analyser was connected to the TEM cell via a coaxial cable, and N-type connectors were designed to match the impedance of these cables, preventing reflections during measurements. The pin at the back of the connector acts as a continuation of the coaxial cable's copper core. To maintain a 50Ω impedance along the entire length of the pin to its connection with the septum, coaxial cable calculations were used to determine the necessary inner diameter of the supporting structures. This inner diameter effectively serves as shielding for the pin, functioning in the same way that the outer shielding protects the copper core in coaxial cables.

The outer diameter of a coaxial cable is given by Equation 3.1: Where Z_0 is the characteristic impedance of the coaxial cable (in ohms), D represents the outer diameter of the cable and in this case the inner diameter of the supports, d is the inner diameter of the cable or in this case the connecting pin of the N-type connector, and ε_r denotes the relative permittivity (dielectric constant) of the insulating material between the inner and outer conductors which in this case is air.

$$Z_0 = 138 \times \frac{\log(D/d)}{\sqrt{\varepsilon_r}} \tag{3.1}$$

That would would yield the following values:

- $Z_0 = 50\Omega$, desired characteristic impedance
- $d = 3$ mm, the diameter of the connecting pin (fig 3.8)
- $\varepsilon_r = 1$, relative permittivity of air

Using the above equation and values, the inner diameter of the supports can be calculated as shown in equations 3.2 to 3.7.

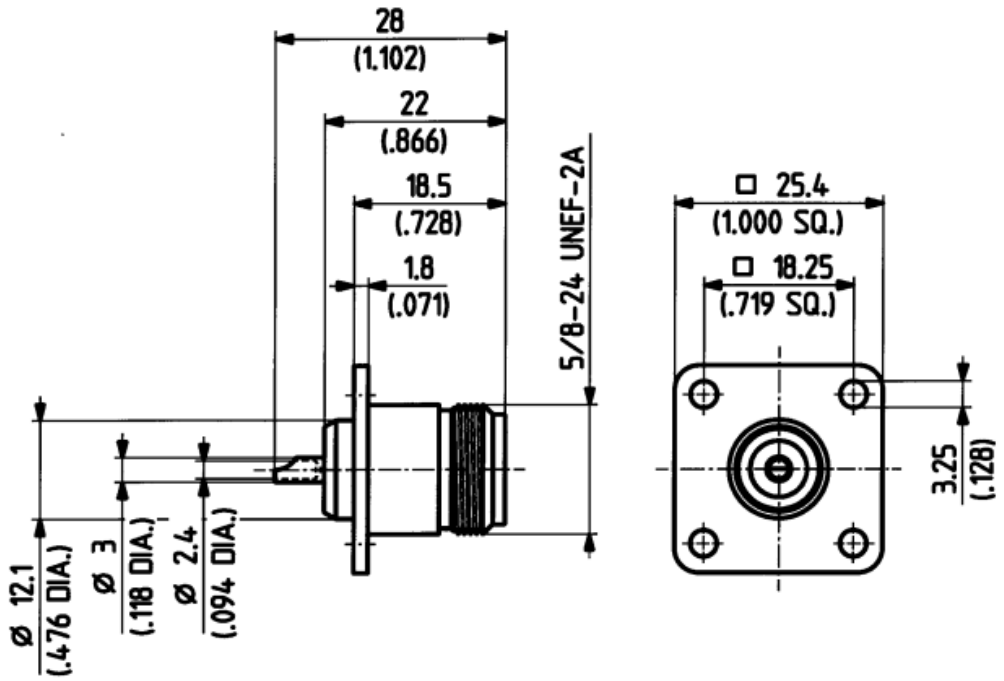

Figure 3.8: Male N-Type Connection

$$\frac{Z_0}{138} = \frac{\log(D/d)}{\sqrt{\varepsilon_r}} \tag{3.2}$$

$$\frac{Z_0}{138} \times \sqrt{\varepsilon_r} = \log(D/d) \tag{3.3}$$

$$10^{\frac{Z_0}{138} \times \sqrt{\varepsilon_r}} = \frac{D}{d} \tag{3.4}$$

$$(10)^{\frac{Z_0}{138} \times \sqrt{\varepsilon_r}} \times d = D \tag{3.5}$$

$$D = (10)^{\frac{50}{138} \times \sqrt{1}} \times 3.04 \tag{3.6}$$

$$D = 7 \text{ mm} \tag{3.7}$$

The depth of the supports in the TEM cell is determined by the length of the connection pin of the N-type connector. As shown in figure 3.8, the connection pin protrudes 6 mm out of the connector itself. This section of the N-type connector was to be soldered to the septum, thereby determining the depth of the support.

After the physical constraints were established and the calculations completed to ensure a 50 Ω impedance, a CAD model was created in CADFEKO to evaluate the EM component of the coax-to-stripline section of the TEM cell. Figure 3.9 on the following page illustrates the developed CAD model.

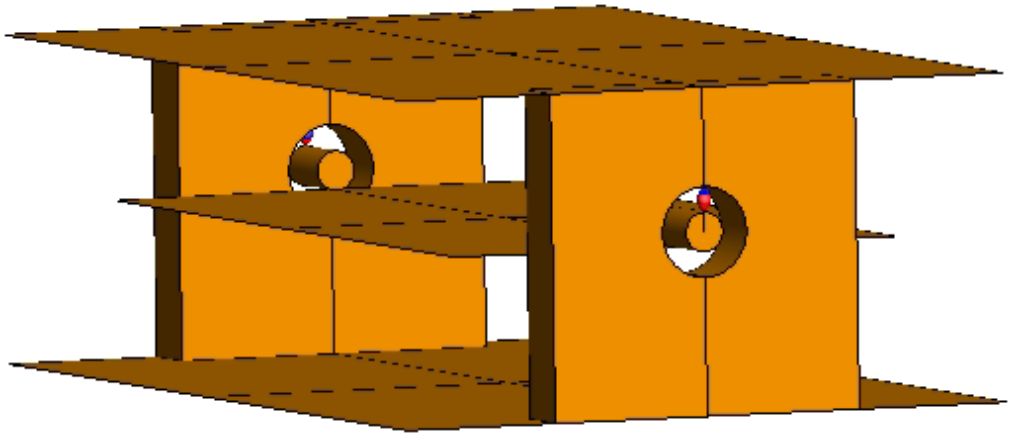

Figure 3.9: Support Offsets

The model was set up to match the expected physical attributes of the coax-to-stripline section as closely as possible. The N-type connector and dummy load used are off-the-shelf items and testing occurred within their specified ranges as indicated by their data sheets in Appendix A.1. Therefore they were assumed to be suitably matched within these ranged and so the simulation was run from the back of each N-type connector on either side. The figure 3.10 illustrates this.

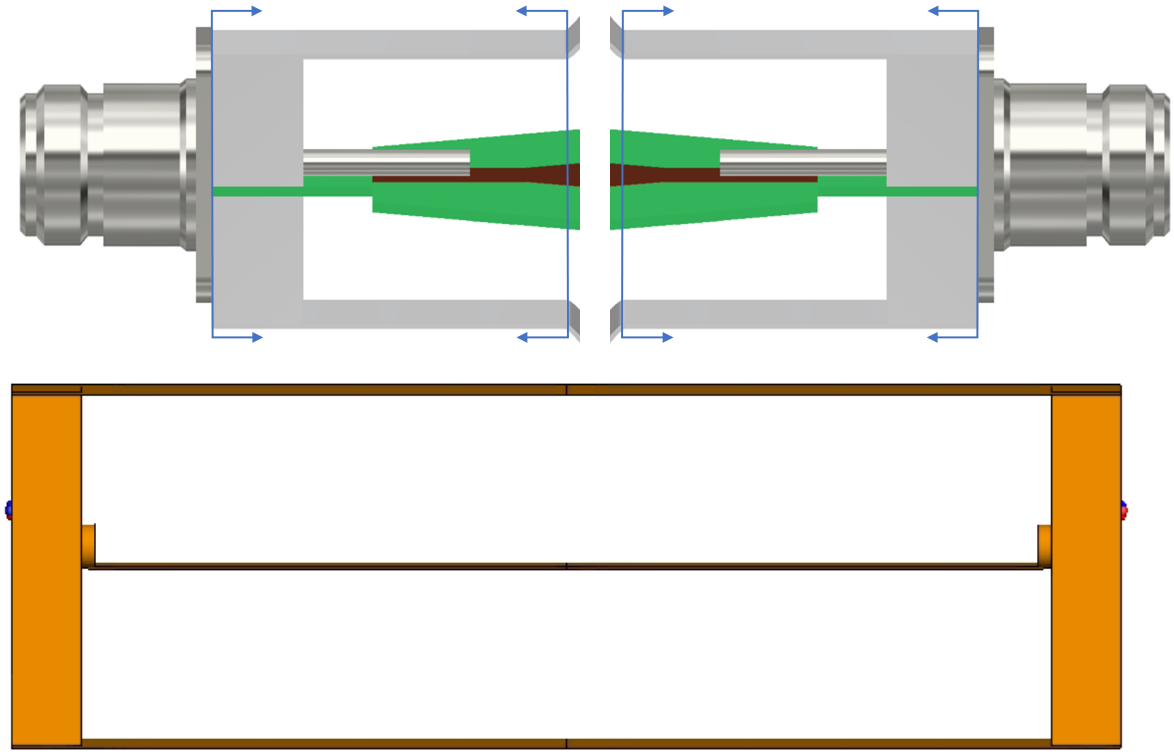

Figure 3.10: Coax-to-stripline Simulation

The calculated and constrained dimensions of this model are shown in figure 3.11. With reference to 3.11a, the height of the connection was chosen to match the height of the N-type connector (25.4 mm), and the depth of the connection was set to 5 mm to ensure sufficient coax coverage for the protruding connection point of the N-type connector, which

is 6 mm. This leaves a 1mm protrusion behind the TEM cell supports to facilitate the connection to the septum. This length is important because the septum cannot touch the supports of the TEM cell, as it will be grounded. If the septum is grounded, no measurement will be possible as the energy of DUT will be shunted to ground.

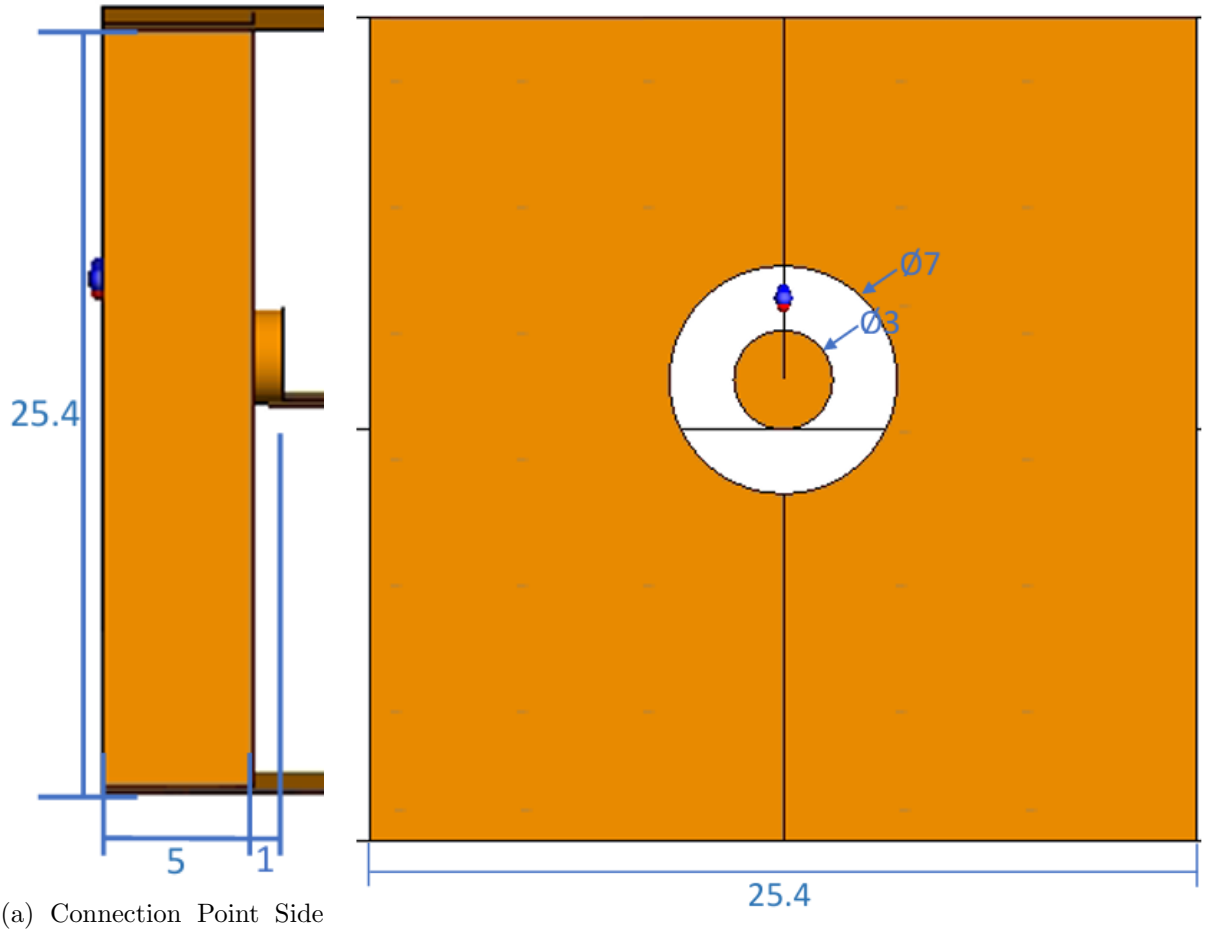

(a) Connection Point Side View

(b) Connection Point Front View

Figure 3.11: Feko CAD Coax-to-Stripline Model Dimensions

Figure 3.11b provides a side view of the coax-to-stripline CAD FEKO model, and the dimensions were chosen as follows. The center point is 3 mm to represent the connection pin on the N-type connector. The outer diameter of the coax section of the design is 7 mm, as calculated in equations 3.2 to 3.7, to ensure a 50 Ω impedance over the coax section of the model. The width of both the TEM cell connector and the mounting plate of the N-type connector is taken to be 25.4 mm.

The dimensions of the stripline section of the model are calculated as follows.

Using the calculations described in Chapter 3, Section 3.7 of *Microwave Engineering*, one can calculate the effective width of the center conductor (W_e) in a stripline using the following formula:

$$\frac{W_e}{b} = \frac{W}{b} - \begin{cases} 0 & \text{for } \frac{W}{b} > 0.35 \\ (0.35 - \frac{W}{b})^2 & \text{for } \frac{W}{b} < 0.35 \end{cases} \tag{3.8}$$

In this equation, $\frac{W}{b}$ is determined using formulas 3.9 and 3.10. The dielectric height between the strip and the ground planes (b) is 25.4 mm as seen in figure 3.11a. The

relative permittivity of the dielectric material (ϵ_r) between the strip and the ground planes is 1 (Air), and the desired characteristic impedance (Z_0) is 50 Ω.

This yields the following:

$$\frac{W}{b} = \begin{cases} x & \text{for } \sqrt{\epsilon_r} Z_0 < 120\Omega \\ (0.85 - \sqrt{0.6 - x} & \text{for } \sqrt{\epsilon_r} Z_0 > 120\Omega \end{cases} \tag{3.9}$$

$$\text{where } x = \frac{30\pi}{\sqrt{\epsilon_r} Z_0} - 0.441 \tag{3.10}$$

Substituting $Z_0 = 50\ \Omega$, $b = 180$ mm, and $\varepsilon_r = 1$ into the above formulas yields:

$$\frac{W}{b} = 1.444, \quad \text{since } \sqrt{\varepsilon_r \times Z_0} < 120 \quad \text{(using 3.10)} \tag{3.11}$$

Then, substituting this value for $\frac{W}{b}$ in formula 3.8, the following is obtained:

$$W_e = b \times \frac{W}{b} \text{where b} = 25.4$$

$$W_e = (25.4) \times \frac{W}{b} = 36.68 \text{ mm} \quad \text{for the connection section of the septum}$$

Again, the parameter b is taken as 25.4 since the height between the ground planes in the stripline section is 25.4 mm as explained previously. This yields a required value of 36.68 mm for the centre conductor of the stripline section of the CAD model. As suggested by the text, the width of the outer ground planes of the stripline is not particularly important as long as it is sufficiently wide. Keeping with stripline design practices, the grounded planes are modelled at a width of 50 mm, as seen in figure 3.12. The ground planes will be altered accordingly after the simulation results are analysed, if necessary.

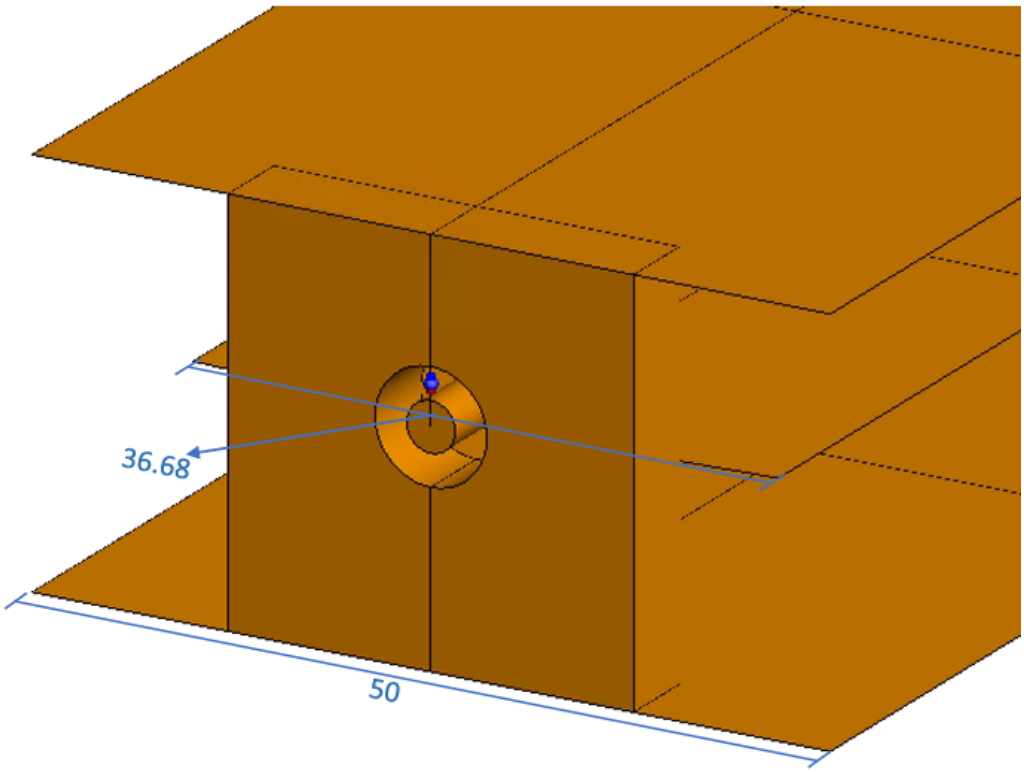

Figure 3.12: Coax-to-stripline Septum Dimensions

After the drawing was effectively modelled, the electrical components were set up. To simulate an electrical signal moving through the modelled figure, a wire port was used, as shown in figure 3.13. Notice that there are two wire ports. One will simulate a signal (SOURCE), and the other will be simulated as a 50 Ω dummy load (LOAD). The blue part of the wire ports indicates the grounded section of the port, while the red part indicates the live part of the signal. The SOURCE port was set up to simulate a 100 MHz - 2 GHz signal.

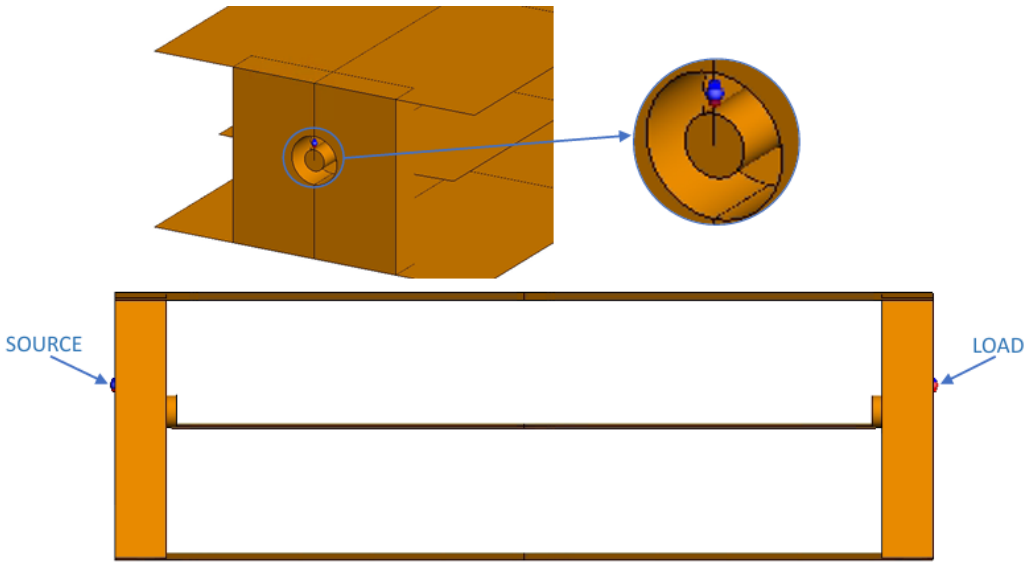

Figure 3.13: Coax-to-stripline Wire Ports

These elements were simulated with the results seen in the figure 3.14 below.

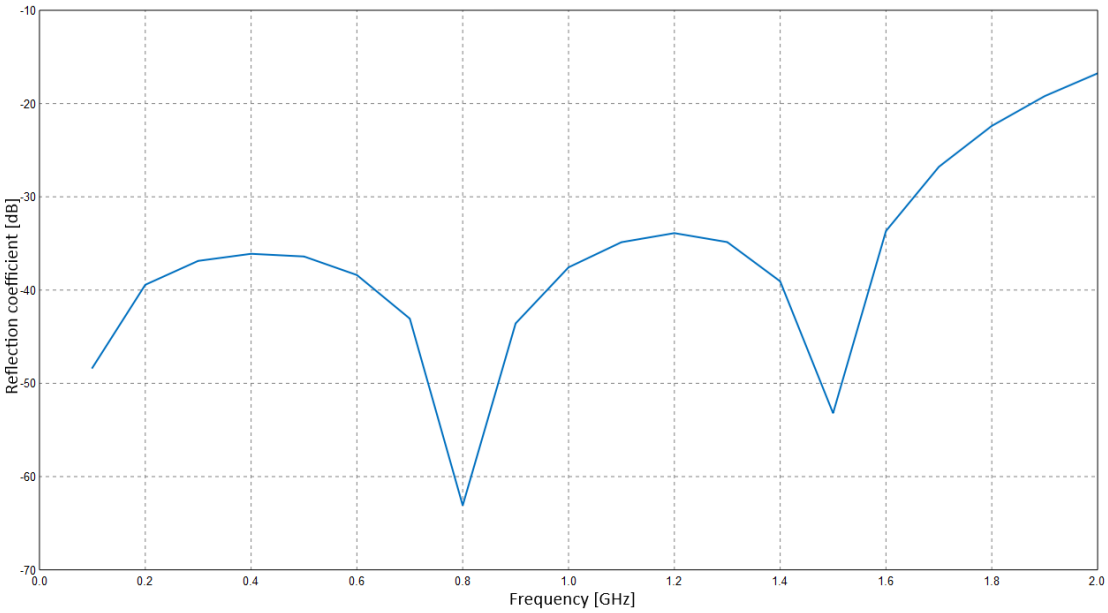

Figure 3.14: Reflection Coefficient of Coax to Strip

Figure 3.14 depicts the reflection coefficient magnitude (in dB) across the same frequency range. The reflection coefficient is a critical parameter for assessing impedance matching, as it indicates the amount of signal reflected back due to impedance mismatches. The results show a reflection coefficient below -10 dB throughout the frequency range, with significant dips observed at several points, indicating excellent impedance matching. Notably, the reflection coefficient remains below -30 dB for most frequencies, with values reaching as low as -60 dB around 0.8 GHz and 1.6 GHz, highlighting regions of exceptionally low reflection and efficient power transfer.

The results align precisely with the project's objectives as outlined in the relevant literature on "Designing Transverse Electromagnetic (TEM) Cell", validating the coax to stripline dimensions chosen. With the impedance closely aligned with the desired reflection coefficient below -10 dB, and therefore proving a 50 Ω impedance across frequencies ensuring minimum reflections. The next steps in the design is the septum and walls.

3.2.4 Septum & Walls

The subsequent design steps involve transitioning from the connection point stripline to the main body of the TEM cell, the widened section of the stripline. This transition includes determining the width and angles of transition from the connector to the central width of the septum and walls, as visually represented in Figure 3.15.

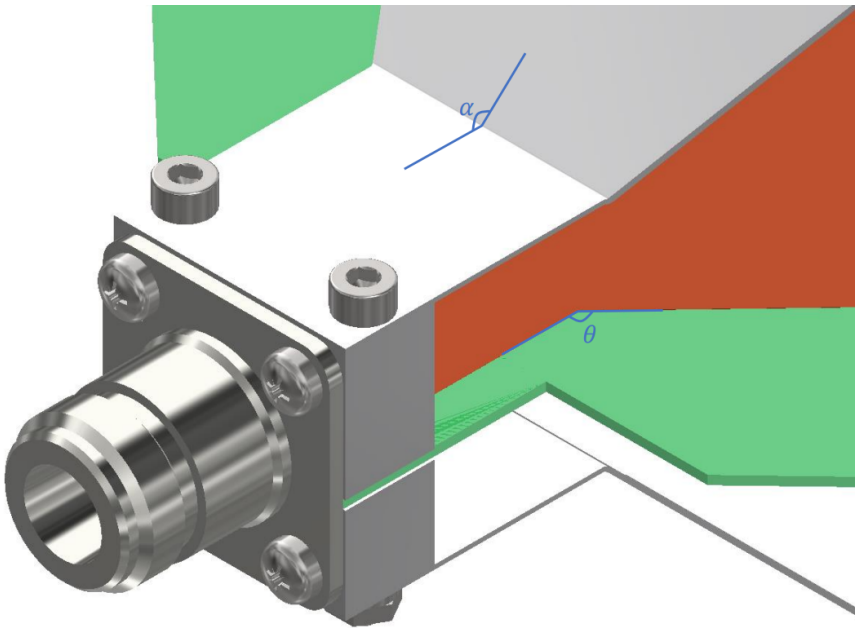

Figure 3.15: TEM Cell Angles

In this phase, the guidance of Sandeep M. Satav 2008 suggests employing a θ angle of 30 degrees. Additionally, the insights from *Microwave Engineering* Chapter 3.7 emphasise that the width of the ground planes, comprising the upper and lower walls of the TEM cell, does not influence the width of the centre septum. Only the height of the wall effects the width of the septum. Consequently, it can be deduced that a consistent value of θ can be used for both the septum as well as the top and bottom walls of the cell.

In simpler terms, as long as the change in septum width corresponds to the change in wall height, the TEM cell will maintain an impedance of 50 Ω. Referring to Figure 3.15, it follows that α equals θ.

Calculating Septum Width

Using the calculations described in Chapter 3, Section 3.7 of *Microwave Engineering*, calculate the effective width of the centre conductor (W_e) in a TEM cell using the following formula as in equations 3.8):

$$\frac{W_e}{b} = \frac{W}{b} - \begin{cases} 0 & \text{for } \frac{W}{b} > 0.35 \\ (0.35 - \frac{W}{b})^2 & \text{for } \frac{W}{b} < 0.35 \end{cases} \tag{3.12}$$

In this equation, $\frac{W}{b}$ is determined using the formulas 3.13 and 3.14. The dielectric height between the strip and the ground planes ((b)) is 180 mm, the relative permittivity of the dielectric material (ϵ_r) between the strip and the ground planes is 1 (Air), and the characteristic impedance (Z_0) is 50 Ω.

$$\frac{W}{b} = \begin{cases} x & \text{for } \sqrt{\epsilon_r} Z_0 < 120\Omega \\ (0.85 - \sqrt{0.6 - x} & \text{for } \sqrt{\epsilon_r} Z_0 > 120\Omega \end{cases} \tag{3.13}$$

$$\text{where } x = \frac{30\pi}{\sqrt{\epsilon_r} Z_0} - 0.441 \tag{3.14}$$

Substituting $Z_0 = 50\ \Omega$, $b = 180$ mm, and $\varepsilon_r = 1$ into the above formulas yields:

$$\frac{W}{b} = 1.444, \quad \text{since } \sqrt{\varepsilon_r \times Z_0} < 120 \quad \text{(using 3.14)} \tag{3.15}$$

Then, substituting this value for $\frac{W}{b}$ in the formula 3.12, the following is obtained:

$$W_e = b \times \frac{W}{b} \text{where b} = 180$$

$$W_e = (180) \times \frac{W}{b} = 259.92 \text{ mm} \quad \text{for the mid section of the septum}$$

It is worth emphasising that the presented equation assumes a centre conductor thickness approaching zero, thereby upholding a consistent fringing capacitance of 0.441. In practical design, a custom PCB can be used effectively as the septum, featuring a centre conductor thickness of 35 µm. Given the significantly reduced thickness (t $\ll$ b) compared to the minimum value of b (180 mm), the condition (t $\ll$ b) is convincingly met. In light of these calculated considerations, the midsection of the TEM cell and the connector segment can effectively be simulated as a stripline. It should be noted that both the upper and lower walls have equivalent dimensions. Using the FEKO optimiser tool, fine adjustments can be made to optimise performance.

Again, CADFEKO software was employed to draw the simulation model using a point-to-point drawing approach. Interconnections were established through variables, where the aforementioned calculations results integrated. This strategic implementation allows for easy and precise modification of the model as required.

The simulation was once again setup with a wire ports as explained in the supports design section. The output obtained in CADFEKO is shown in Figure 3.16 below.

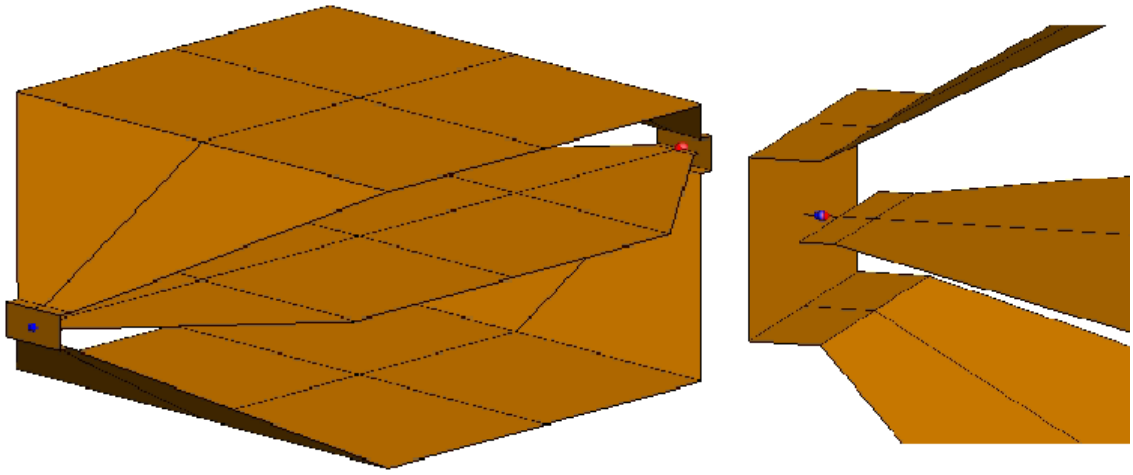

Figure 3.16: Simulation: Strip To Wide Stripline (STWS)

The analysis of simulation results, in figure 3.17, offers insights into the performance of the CADFEKO model illustrated in Figure 3.16. Despite a minor deviation from the target value (below -10 dB), the overall outcome remains predominantly favourable, as indicated by the green curve. This slight variance, however, holds potential significance within the scope of the intended design integration in the next step.

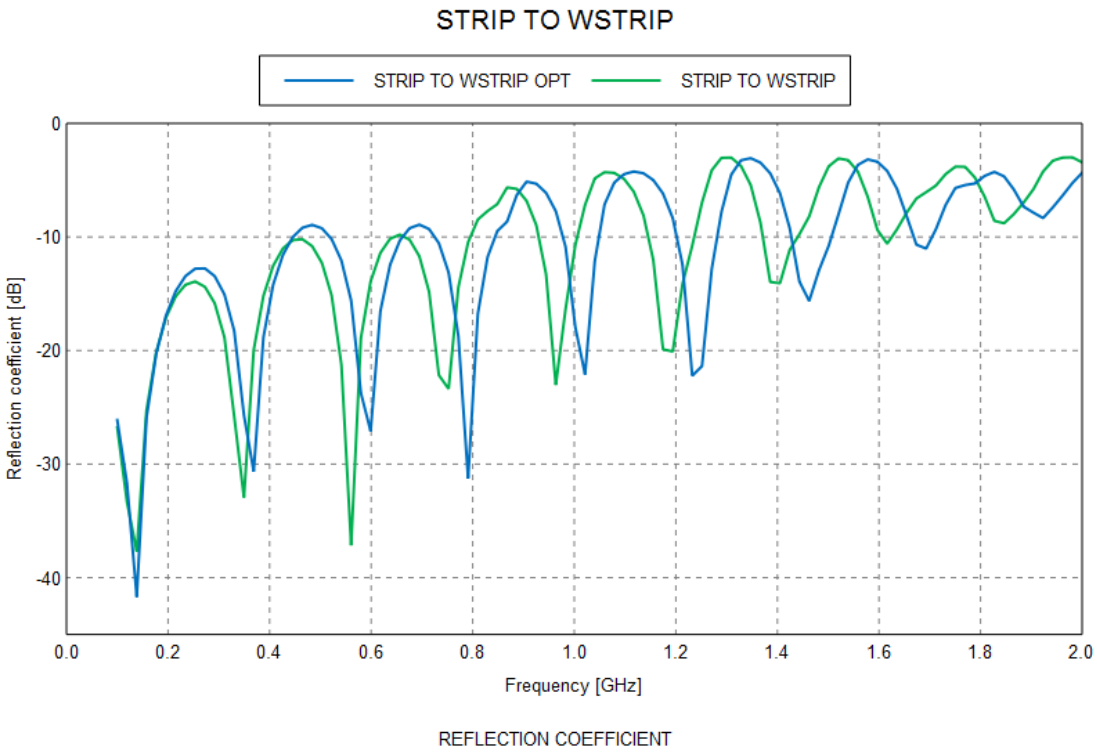

Figure 3.17: Simulation: STWS Optimization Setup and Result

The design amalgamation entails merging this design with the preceding one depicted in figure 3.14. It is expected that this integration will result in an outcome more closely aligned with the desired target since in the current design the transition from coax to stripline is not modelled properly.

To further refine the design, the FEKO OPTIMISER tool was utilized to optimize key structural parameters. The optimisation objective was to minimise the magnitude of the reflection coefficient (Snn) to improve impedance matching. As shown in the optimisation setup in Figure 3.18, the two variables selected for optimisation were the distance between the two planes of the walls in the middle and the distance between the two planes of the walls at the connection points, both of which were varied to achieve optimal performance. The optimisation did not use a mask and was configured to minimise the magnitude of the reflection coefficient directly.The optimization result was, rounded up, 95mm and 35mm respectively. This was applied to the CADFEKO model and reevaluated. The results of this optimization process is shown in figure 3.17 depicted by the blue line. As can be seen, the change did not make any significant difference to the result. A better design cannot be discerned from this results and both therefore both measurements must be evaluated in the final experiment to see if a discernible difference arises.

3.2.5 TEM Cell Model Simulations

Taking into account the simulated results of the connection point (3.2.3) as well as the septum and walls (3.2.4) presented in these sections, they can now be amalgamated into a unified design with the expectation of obtaining satisfactory results. The rationale behind isolating these specific sections was to evaluate the optimal calculation at critical junctures, focusing primarily on potential failure points, notably the coax to stripline transition (Section 3.2.3) and the stripline to widened stripline transition (Section 3.2.4).

```
SIMPLEX NELDER-MEAD finished
Maximum number of analyses reached: 20

Sensitivity of optimum value with respect to each optimisation parameter:
  Parameter                      Sensitivity
  cen_wal_h                      2.413368309e-02
  con_wall_h                     7.705568919e-03

Optimum found for these variables:
  cen_wal_h                    =   9.457586024e+01
  con_wall_h                   =   3.548845575e+01
Optimum aim function value:   6.500537040e+00
```

Figure 3.18: Simulation: STWS Optimization Results

With the results gathered from these tests, a full TEM cell simulation could be put together in CADFEKO. This was relatively straight forward, the dimensions of each calculated components was taken and a new CAD model was developed with wire ports. The amalgamation can be seen below in figure 3.19 below.

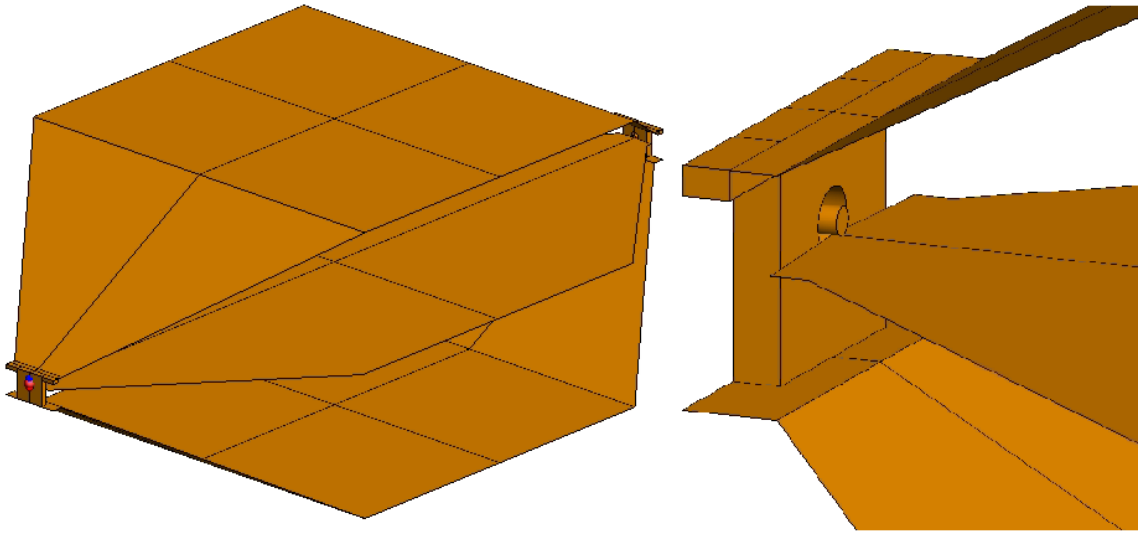

Figure 3.19: Simulation: TEM Cell CADFEKO

The simulation yielded very promising results, as can be seen in the figure 3.20 below.

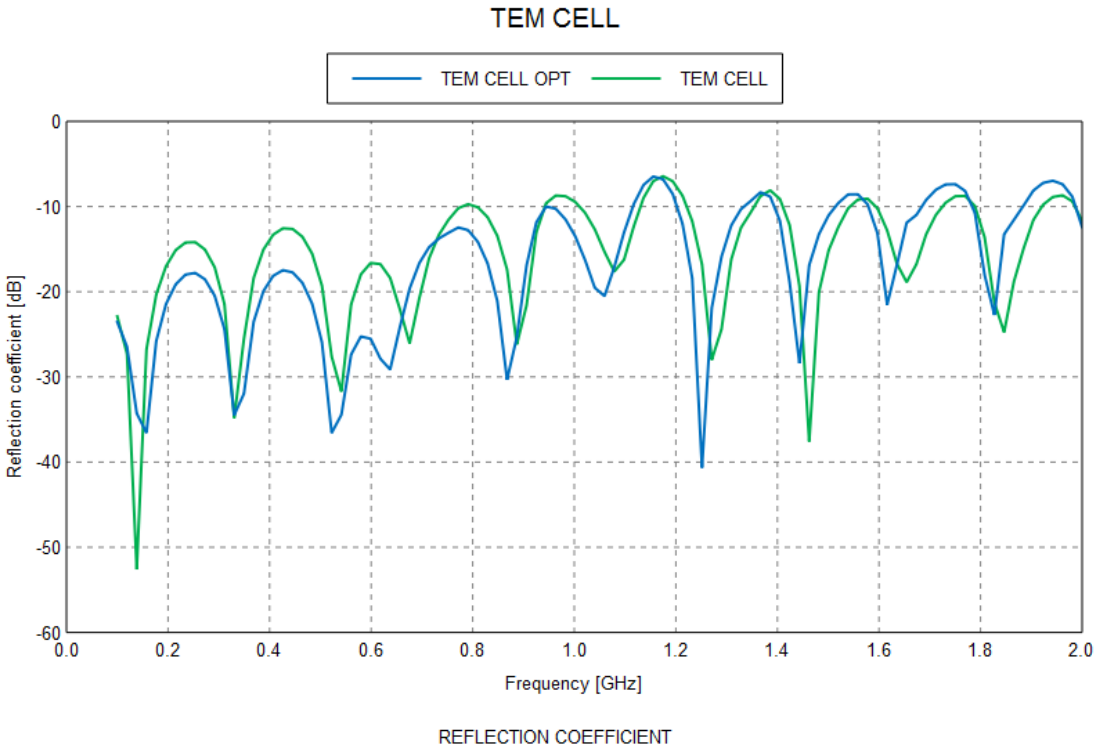

Figure 3.20: Simulation: TEM Cell Simulation Results 1

The results in figure 3.20 depicts an analysis of the reflection coefficient for the full CAD model of the TEM cell, comparing the optimized design (TEM CELL OPT) with the initial design (TEM CELL). The reflection coefficient, plotted over a frequency range from 0 to 2 GHz, indicates the effectiveness of impedance matching for the TEM cell design.

As shown in Figure 3.20, the reflection coefficients for both the optimized (blue curve) and initial designs (green curve) generally stay below -10 dB across most of the frequency range. This reflects good impedance matching, which is essential for minimizing signal reflections and ensuring efficient signal transmission. The significant dips below -30 dB observed at several frequencies highlighting regions of particularly low reflection and excellent impedance matching.

A closer examination reveals that the optimized design (TEM CELL OPT) exhibits better performance, with more pronounced dips and lower reflection coefficients at various frequencies compared to the initial design. For instance, around 0.2 GHz, 0.8 GHz, and 1.6 GHz. Although the unoptimized design achieves a reflection coefficients as low as -50 dB, it is the only significant better results compared to the optimized output. Therefore the optimized result is the better choice for design because of the more consistent performance across the entire frequency range.

The observed behaviour, with reflection coefficients well below the acceptable threshold of -10 dB, confirms the suitability of the TEM cell design for practical applications. This level of impedance matching ensures that very few frequencies are out of range and thereby providing a very small error margin, perfect for pre-compliance testing.

3.2.6 Support Design Review

The supports required modification to accommodate the additional screws necessary for the assembly of the walls and septum to create the final product of the TEM cell. The

initial calculated size of the supports aligned well with the requirements of EMC, but will pose challenges during assembly. An extended section was necessary to facilitate the final assembly, but this extension had to be executed in a manner that minimally affected the characteristic impedance properties of the connection section of the TEM cell. Equation 3.6 played a critical role in guiding these modifications, indicating that the diameter of the coaxial part of the connector should remain at 7mm, unaffected by external alterations to the supports. Similarly, equation 3.13 highlighted that the width ((W)) and height ((b)) of the connection section, crucial for the stripline, should remain unchanged. Therefore, the adjustments were focused on the upper half of the supports in an attempt to not affect the positive simulations results already obtained. The new design is as in figure 3.21 below providing the necessary space to mount the screws for assembly.

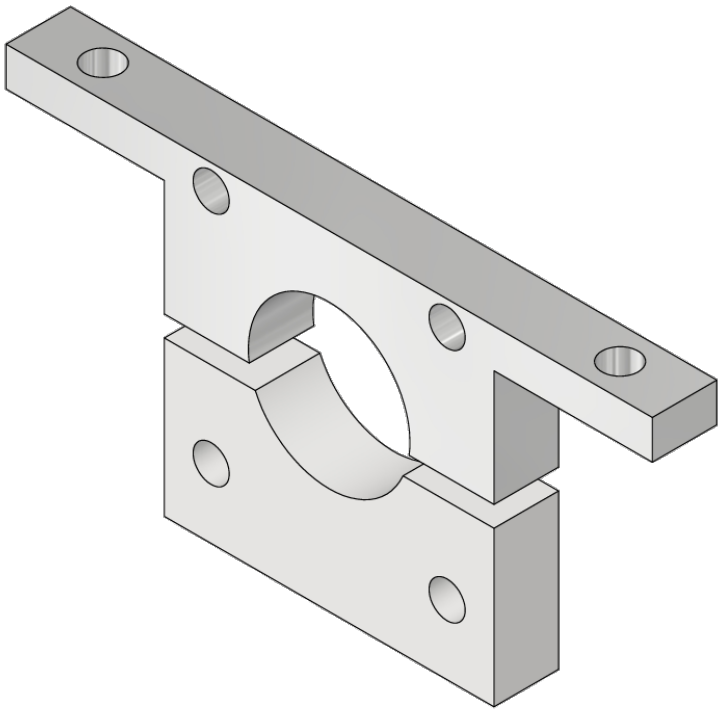

Figure 3.21: Supports Final Design

3.2.7 TEM Design Review

After adjustment of the supports was made, the rest of the TEM cell required a thorough reevaluation. The dimensions of the cell presented so far were theoretically calculated to ensure a characteristic impedance of 50 ohms over the desired frequency range. However, these precise theoretical values are often impractical for manufacturing and need to be adjusted accordingly. Fortunately, the simulated data confirmed that our theoretical dimensions achieved the desired impedance. Hence, minor adjustments were made to these theoretical dimensions to align with manufacturability, followed by subsequent simulations. The key design changes as seen in section 3.4 and their subsequent simulations were as follows:

- Wall Connection Point Width: Adjusted to 50 mm
- Wall Connection Point Depth: Adjusted to 10 mm
- Wall Wide Width: Adjusted to 350 mm

- Wall Wide Depth: Adjusted to 300 mm

The resulting CADFEKO model reflecting these new dimensions is depicted in Figure 3.22.

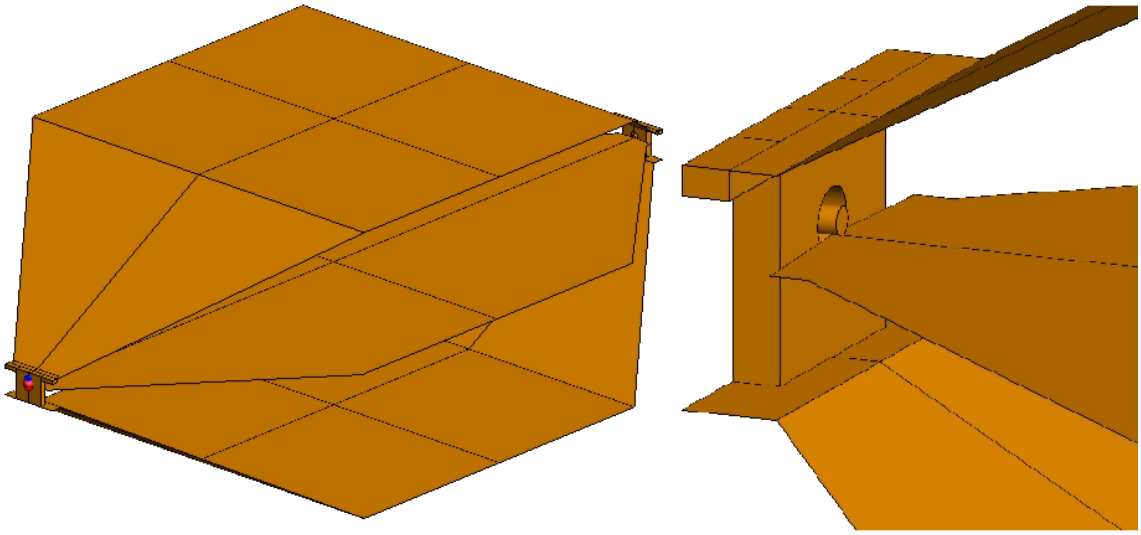

Figure 3.22: Simulation: TEM Cell Final CADFEKO

Upon simulation with these new dimensions, the following results were obtained, as shown in Figure 3.23.

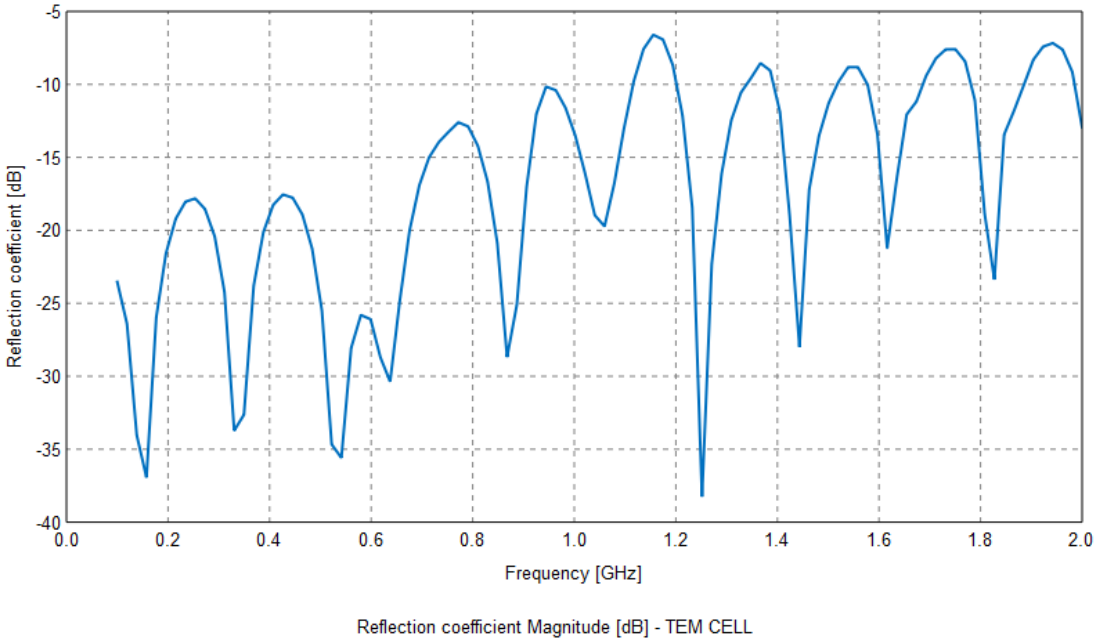

Figure 3.23: Simulation: TEM Cell Simulation Results 2

As these result closely match that of the result in in figure 3.20, it is safe to say that the change in support design and dimensional updates did not effect the impedance of the TEM cell and can still be calcified as sufficiently matched. Now that the design has a sufficiently low margin of reflection, one more test can be conducted before the design procedure can begin.

3.3 Field Uniformity

Field uniformity testing is crucial in EMC testing, as it ensures that the DUT is exposed to a consistent and repeatable electromagnetic field across its surface to insure accurate measurements of the RE. A consistent field enables compliance with international standards, improves the reproducibility of test results, and simplifies the identification of any variability across the DUT. By reducing inconsistencies in the testing setup, field uniformity testing enhances both the efficiency and validity of EMC assessments.

TEM waveguides, particularly TEM cells, are central to EMC testing as they provide a controlled, uniform field environment for pre-compliance testing. However, achieving a consistent electromagnetic field distribution within a TEM cell presents challenges, with field inhomogeneities potentially impacting the reliability of test results. To address this, standards like IEC 61000-4-20 define field uniformity criteria, setting maximum allowable standard deviations for field values across a grid of at least 5 test points. The testing procedure outlined in IEC 61000-4-20 involves measuring the electric field strength at multiple points within the test volume to evaluate the uniformity of the electromagnetic field. These measurements are taken over a range of frequencies, and deviations are assessed to ensure compliance with uniformity requirements. The acceptable limits of these values in the standard are derived from statistical analyses of field variability and its effect on EMC test repeatability. By enforcing these limits, the standard ensures that variations in field distribution do not introduce significant errors, thereby improving the reliability and consistency of compliance testing.

According to IEC 61000-4-20, the maximum standard deviation for field uniformity is limited to $s_M = 2.61\,\text{dB}$ when the non-uniformity tolerance L is 6 dB, based on a probability factor p of 0.75 with a coverage factor $k(p) = 1.15$ under normal distribution assumptions. This relationship is expressed as follows:

$$s_M = \frac{L}{2k(p)} = \frac{6}{2 \times 1.15} = 2.61\,\text{dB} \tag{3.16}$$

The value of s_M is specified by the standard, but calculated values from field strength data were obtained using "The Statistical Field Uniformity Criterion in Transverse Electromagnetic Waveguides". This article applies statistical analysis to calculate the mean and standard deviation of a data set using the exported data from a simulated field uniformity test of the same CADFEKO model that passed the matching tests in section 3.2.5. The first step is to set up a test area for simulation, as shown in figure 3.24. The test area size is related to the usable test region (one-third of the distance from the bottom wall to the septum) and the anticipated test area of the DUT—in this case, a 10x10 cm CubeSat subsystem. This setup provides the cubic test area depicted in figure 3.24.

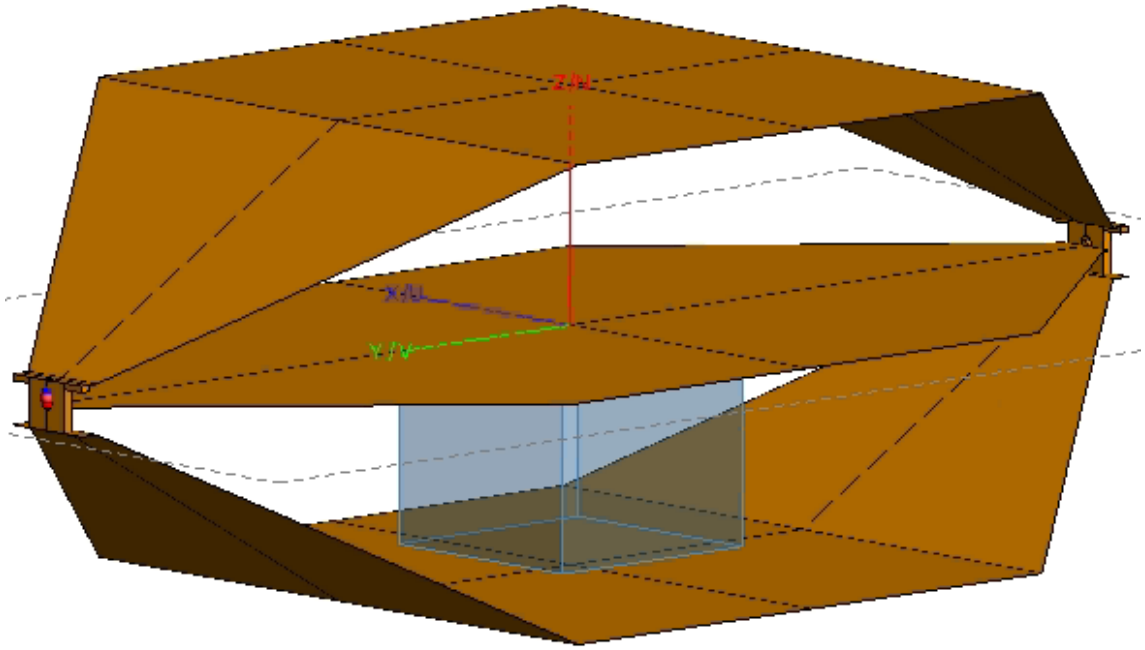

Figure 3.24: Simulation: TEM Cell Field Uniformity Testing Area

The IEC 61000-4-20 standard requires at least 5 test points; however, this simulation uses 143 points for increased accuracy, possible due to the computational power of Feko simulations. After running the simulations, the data are displayed as shown in figure 3.25, which is a heat map of the E-fields on the XZ planes at Y position 0.03 m at a frequency of 1.085 GHz.

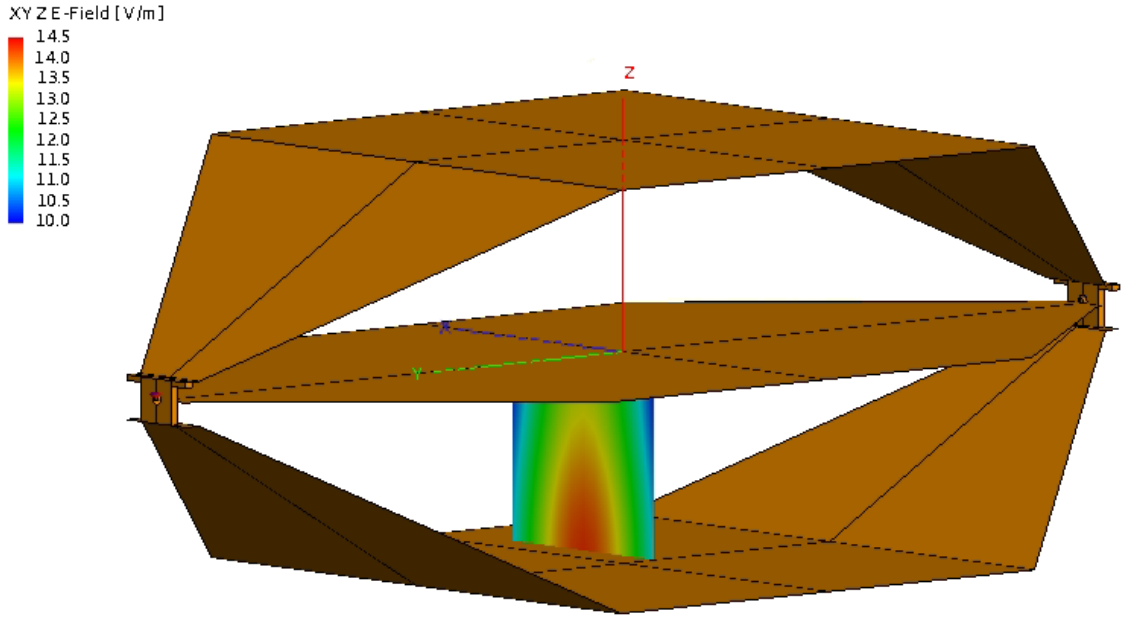

Figure 3.25: Simulation: TEM Cell Field Uniformity Testing Results

The exported data from these simulation are then used to calculate the mean values and standard deviation across the frequency range to determine the field uniformity. The sample mean is calculated using equation 3.17.

$$\bar{e} = \frac{1}{n} \sum_{i=1}^{n} e_i \tag{3.17}$$

Here, $\bar{e}$ represents the mean value, with n as the number of values, following the standard approach for calculating a mean. The mean values in this analysis represent the magnitudes of the E-field at each sampled point, without considering phase or directional vector components. It is calculated for each Y-position plane at each frequency in Matlab. In this setup, the 3D simulation area is sliced into 13 XZ planes, each shifted by 0.01 m on the Y axis, so the full volume is calculated and graphed. The Matlab code calculates the mean E-field value for each Y-plane position (e.g., -0.06 m) at each frequency (starting from 10 MHz), plotting each until reaching 2 GHz. This iterative process repeats for each Y position, resulting in a graph showing all Y positions as well as mean values for E-fields across frequencies.

Following "The Statistical Field Uniformity Criterion in Transverse Electromagnetic Waveguides", after calculating the mean, we use equation 3.18 to determine the standard deviation:

$$s = \sqrt{\frac{1}{n-1} \sum_{i=1}^{n} (e_i - \bar{e})^2} \tag{3.18}$$

Here, s is the standard deviation, n is the number of data points, e_i represents each individual data point, and $\bar{e}$ is the mean of the dataset being evaluated. Standard deviation provides a measure of how much the data are dispersed around the mean. This is extremely useful in this context, as we seek to understand the standard deviation from the mean for each frequency at a specific Y position within the 3D simulated volume to assess if it falls within the allowable restrictions placed by the IEC standards. Once the sample mean and standard deviation have been calculated, the plots below can be analysed.

3.3.1 Analysis of Y-Position Mean Values vs. Frequency

The first graph, shown in Figure 3.26, illustrates the variation in the electric field mean values across a range of frequencies at different Y-positions within the TEM cell. Each line represents the mean E-field at a specific Y-position and frequency, providing insight into the field's spatial distribution and frequency response. Across most of the frequency range, the E-field values remain relatively stable, indicating a level of uniformity in field distribution. However, significant peaks can be observed around 1.5 GHz and 1.8 GHz, suggesting areas where the field strength is substantially more scattered. These peaks indicate frequencies where the E-field deviates notably from the overall mean values, potentially leading to non-uniformity in the field distribution across the measurement plane.

The overall mean value is obtained by calculating the mean of all of the plot data to see how much the plot is scattered from its mean value. In the context of TEM cell design, ensuring field uniformity is essential to obtain accurate measurements of the DUT, as inconsistencies in the field can lead to inaccurate assessments of the DUT's response.

The observed peaks at 1.5 GHz and 1.8 GHz may indicate the presence of higher-order modes, such as the TE_{10} mode, within the TEM cell. A pure TEM mode produces a uniform field, but at higher frequencies, higher-order modes can emerge, resulting in localized variations in field strength. These variations align with what would be expected when multimodal effects begin to influence the field distribution. This suggests that at

certain frequencies, the field uniformity is naturally affected by multimoding, which is a known characteristic of TEM cells beyond their fundamental operating range. However, to fully assess whether these variations pose a significant issue, the standard deviation of the E-field values is evaluated in the next section.

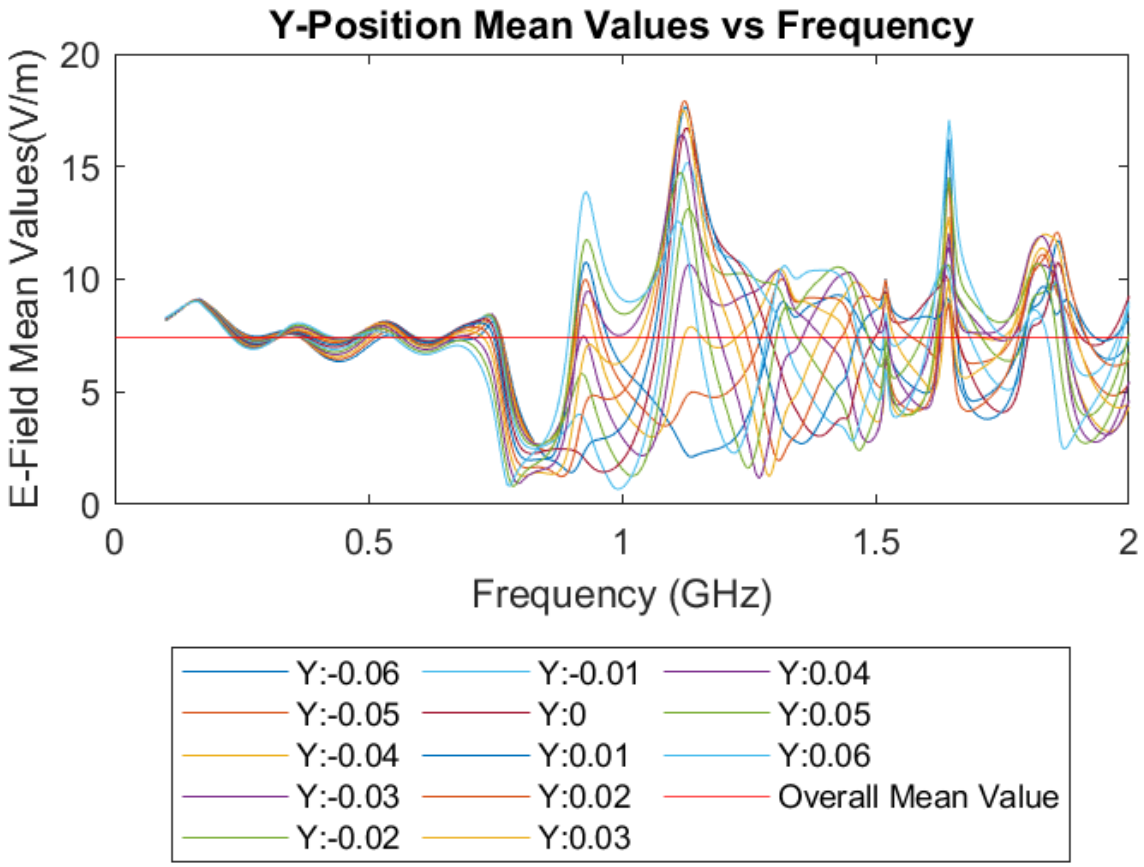

Figure 3.26: E-field Means

3.3.2 Analysis of Y-Position Standard Deviation vs. Frequency

The second graph, shown in Figure 3.27, displays the standard deviation of the E-field at each frequency across the specified Y-positions, highlighting the degree of field uniformity. The red line represents the maximum allowable standard deviation $s_M = 2.61\,\text{dB}$ to maintain measurement accuracy. Peaks in this graph indicate frequencies where field non-uniformity is higher, exceeding the acceptable deviation threshold, particularly above 1.5 GHz. These problem frequencies pose a challenge to maintaining a stable and uniform field within the TEM cell, as high standard deviations imply fluctuations from the mean E-field values. For accurate DUT evaluation, the field should remain uniform uniform. However, this graph displays a lot of data which makes it difficult to really understand how much of the test area does not conform to the IEC field uniformity standards. The third graph helps do better understand represent this.

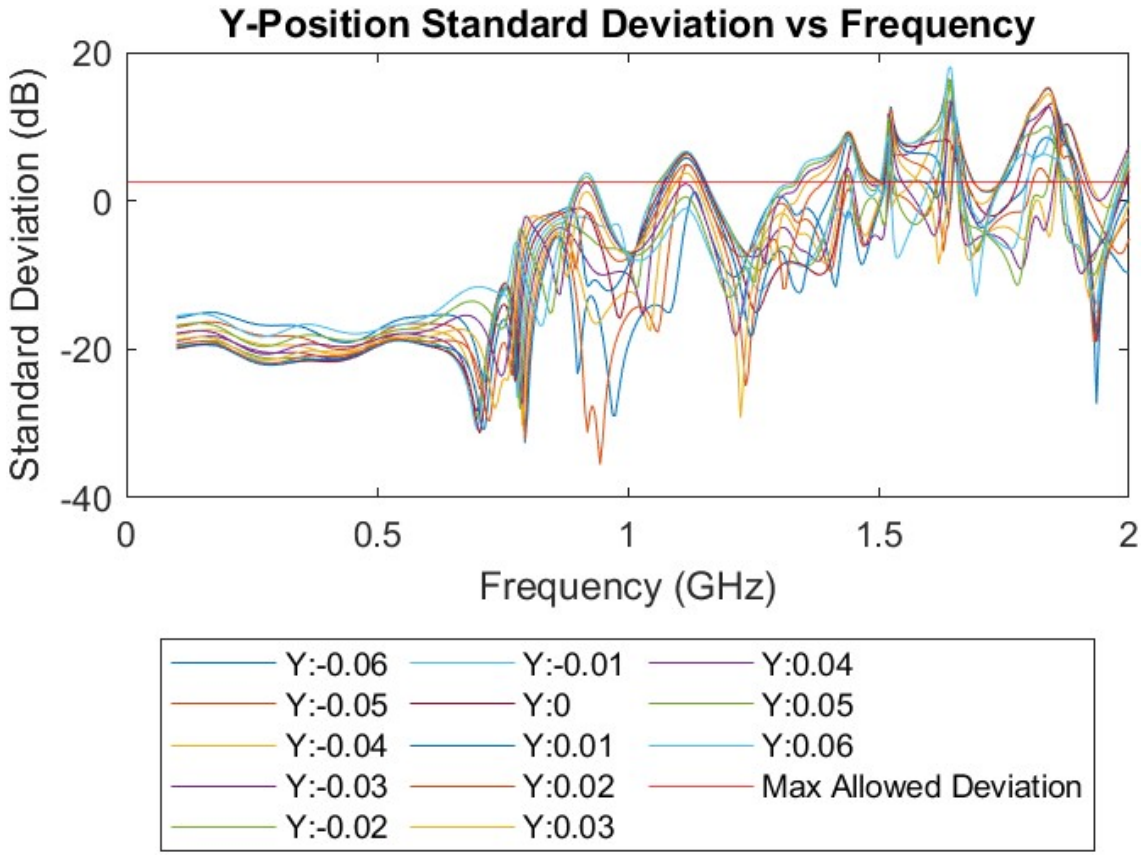

Figure 3.27: Standard Deviation

3.3.3 Analysis of Percentage Above Allowable Standard Deviation per Y-Position

The third graph, shown in Figure 3.28, presents the percentage of E-field values at each Y-position that exceed the allowed standard deviation threshold across various frequencies. This plot summarizes the field's reliability over the entire frequency range, with the red line marking the maximum percentage observed in this dataset.

At its highest point, the deviation reaches 25.91%, occurring predominantly in the upper frequency range of the measurements. While this percentage is relatively high, it represents the worst-case scenario at a specific frequency rather than the overall field behaviour. The majority of the lower frequency range remains well within the acceptable standard deviation limits, indicating that for most of the operational range, field uniformity remains sufficiently stable for pre-compliance.

Although the IEC standard requires that the maximum standard deviation not be exceeded for full compliance testing, this result remains suitable for pre-compliance testing, where the primary goal is to evaluate frequency-dependent field behaviour and identify potential non-uniformity effects. This plot can therefore serve as a reference to determine frequency ranges where field reliability is higher, allowing for targeted adjustments in testing procedures if necessary.

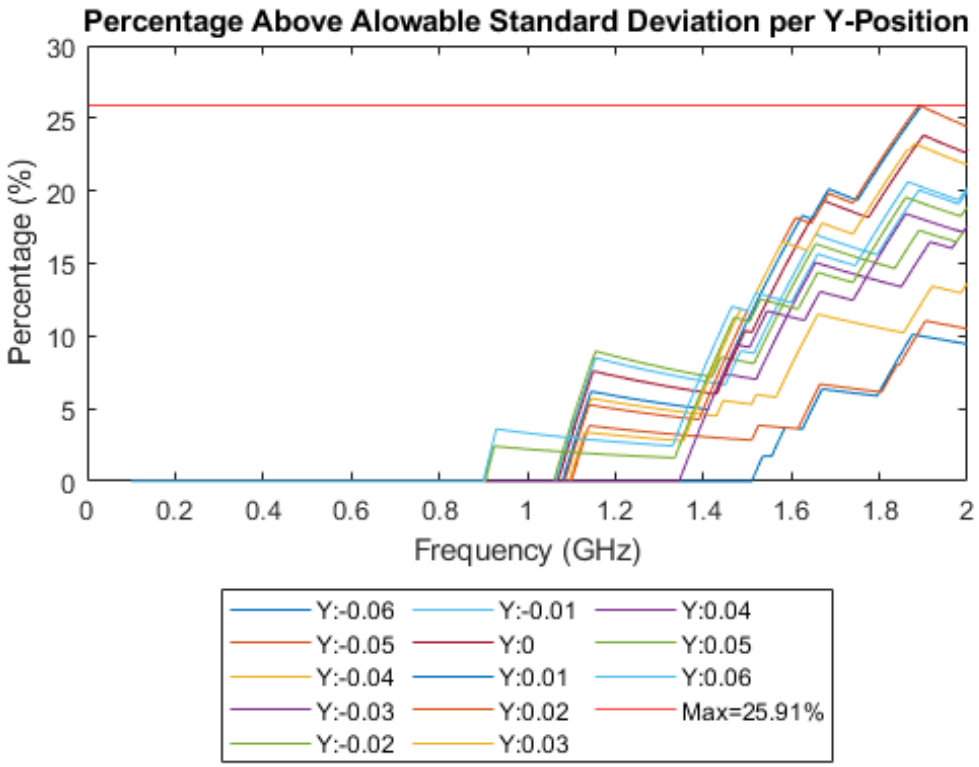

Figure 3.28: Percentage Values Above Allowable Deviation

3.4 Manufacturing and Fabrication of the TEM Cell

The design drawings were drawn using AUTODESK Inventor. Each part was drawn separately, incorporating the dimensions obtained through the procedure outlined in the preceding sections. Subsequently, the individual part files were assembled into an assembly drawing, as illustrated in Figure 3.29.

To exemplify the DIY nature of this project, the fabrication of each component was to be done using campus resources wherever feasible. The technical team at CPUT confirmed that this was possible with the on campus equipment and resources. However, given time constraints arising from student strikes and material availability issues, manufacturing of these parts had to be outsourced to TFDesign.

Consequently, alternative materials were used. While the original plan intended to utilize FR-4 PCB for the septum, logistical constraints necessitated a last-minute change to aluminium. Adjustments were made to the design to accommodate this alteration. Despite these challenges, the fabrication proceeded with the utmost diligence and adherence to the project's objectives.

The walls and septum were made from 1.6mm aluminium sheets, water jet cut, and then bent to conform to the specifications outlined in the drawings. The supports were manufactured by laser cutting stainless steel, ensuring their strength and durability.

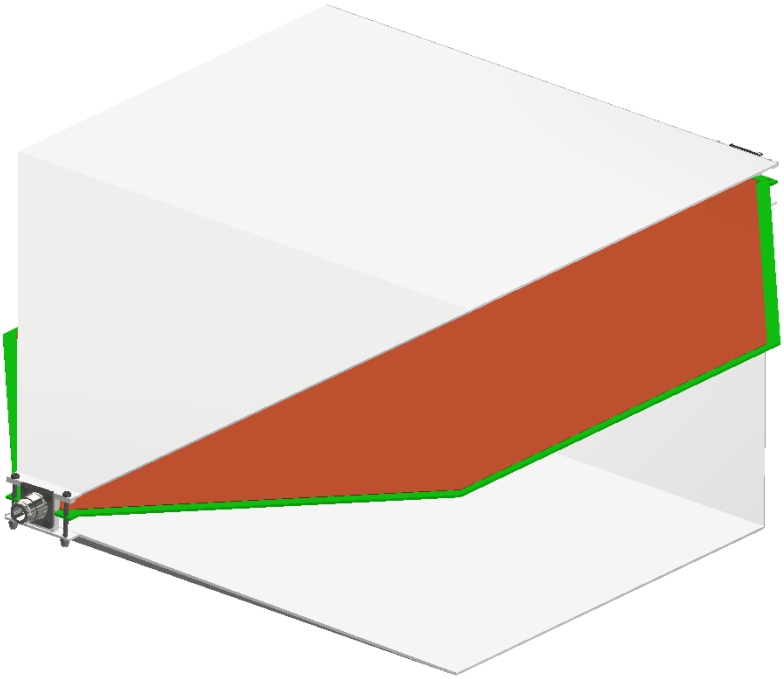

Figure 3.29: Simulation: TEM Cell Assembly Render

3.5 Assembly

Due to the change in material for the septum, it was not as rigid as originally planned. Consequently, special supports were 3D printed with minimal infill to minimize EM interference. This solution is depicted in the figure 3.30 below.

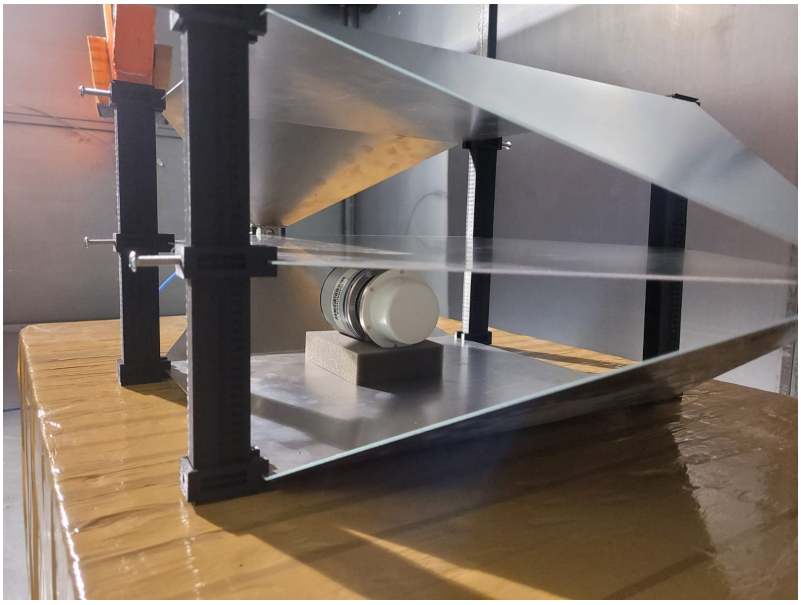

Figure 3.30: TEM Cell Assembly with Supports

Chapter 4

Verification Testing

4.1 Simulation Data

To evaluate the overall success of the project, the measured data is compared to the simulated data to determine the feasibility of replicating the design and build procedure for a TEM cell with narrower or more focused measurement capabilities.

4.2 Evaluation Criteria

The purpose of this chapter is to present the results and analysis of the developed TEM cell. This section details the evaluation process, including the testing procedures and validation criteria used to ensure the TEM cell's performance and reliability. The chapter is divided into several key sections, each addressing specific aspects of the testing and analysis.

4.2.1 TEM Cell Evaluation

The TEM cell was evaluated within the 10 MHz to 2 GHz frequency range. The primary components used in the measurement setup included a Comb Generator (CG), Vector Network Analyser (VNA), Spectrum Analyser, Reverb Chamber, Dummy Load, and the fabricated TEM cell itself. The specific connections made during the testing are outlined, ensuring accurate data collection.

Testing Procedures

The testing procedures were designed to thoroughly assess the TEM cell's performance. Initial calibration of the VNA ensured accuracy and reliability of the subsequent measurements. The testing began with spectrum analyser measurements to evaluate the radiated emissions of the CG within the reverberation chamber, both with and without the TEM cell. These measurements provided a baseline for comparison and validation.

Measurements were conducted with the TEM cell connected, with and without the chamber stirrer active, to simulate different operational environments and identify any susceptibility to external noise. The TEM cell's response was evaluated by rotating the device under test (DUT) to four different angles: 0°, 90°, 180°, and 270°. This comprehensive approach ensured that the impact of the DUT's orientation on test results was thoroughly analysed.

Validation Criteria

Validation of the TEM cell's performance was based on several criteria. The primary focus was on maintaining an impedance of 50 ohms and ensuring minimal reflection, measured by the S_{11} parameter. The S_{11} measurements were taken inside and outside the shielded chamber, with the CG both active and inactive. The validation criteria also included comparing the measured data against simulation results obtained from CADFEKO to ensure consistency and accuracy.

The criteria for successful validation included:

Impedance Matching: Ensuring the reflection coefficient remained below -10 dB across the specified frequency range, indicating good impedance matching and minimal signal reflections. Noise Isolation: Assessing the TEM cell's susceptibility to external noise and implementing noise isolation measures where necessary to improve measurement accuracy. Frequency Response: Evaluating the TEM cell's performance across different frequencies, with a particular focus on maintaining accuracy in both high and low-frequency ranges. Replication of Results: Demonstrating that the developed TEM cell could replicate the results obtained from simulations, thereby confirming the reliability of the design and testing methodology. The results of these measurements and their analysis are presented in the subsequent sections, providing a comprehensive evaluation of the TEM cell's performance and highlighting areas for potential improvement.

4.3 TEM Cell Evaluation

4.3.1 Equipment

The test setup was designed to evaluate the accuracy of the TEM cell in the 10MHz-2GHz frequency range. The components used in the measurement setup included:

- A CG, figure 4.4a
- Vector Network Analyzer (VNA) (SubMiniature version A, 100 kHz – 18 GHz, 2-Port), figure 4.4b
- Spectrum Analyser (Tektronix RSA5115B), figure 4.4c
- Reverb Chamber (Width = 2.8 m, length = 5.35 m, height = 2.1 m with Lowest Usable Frequency (LUF) 181.27 MHz), figure 4.4d
- Dummy Load, figure 4.2b
- Fabricated TEM Cell, figure 4.2c
- Chamber Stirrer, figure 4.2d

Connection

The connections made on each end of the TEM cell were to the analyser (Figure 4.4c) and the dummy load (Figure 4.2b). The spectrum analyser was connected to the TEM cell via an N-type connector, as depicted in figure 4.3a. It was assumed that the connector did not have a discernible impact on the analysis and was not compensated for in the analysis.

Furthermore, the N-type connections were soldered to the TEM cell for both the dummy load and analyser. This process was slightly more challenging due to the required design changes mentioned previously. Since the septum was now fully aluminium, the solder

(a) Comb Generator

(b) VNA

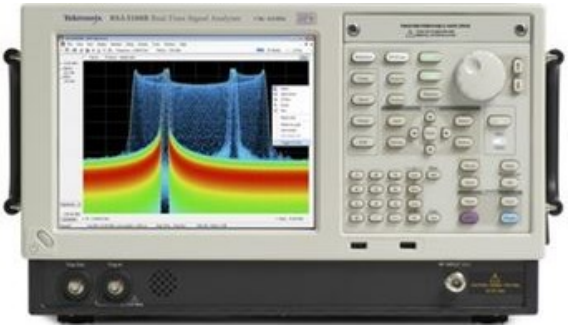

(c) Tektronix RSA5115B

Figure 4.1: Analysis Equipment

(a) Chamber

(b) Dummy Load

(c) Fabricated TEM Cell

(d) Stirrer

Figure 4.2: Testing equipment

(a) Connection to Analyser

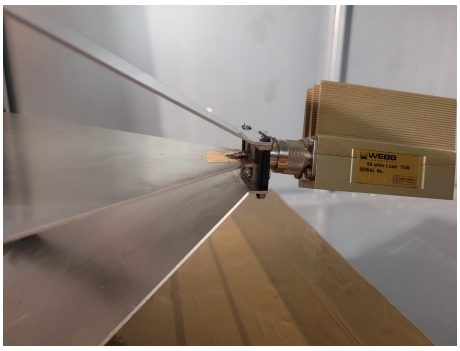

(b) Connection to Dummy Load

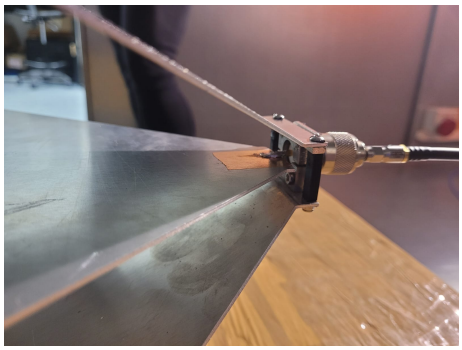

(c) Copper Tape

Figure 4.3: Connections

tended to pull away from the connector. To enhance the bond of the solder to the septum, small pieces of copper tape were used, as shown in figure 4.3c.

4.3.2 Measurement Procedures

Firstly the VNA was calibrated before the measurements were performed to ensure accurate and reliable results. In summary, spectrum analyser measurements were performed to assess the radiated emissions of the CG within the reverberation chamber, both with and without the TEM cell present. Additionally, measurements were conducted with the TEM cell connected but with the stirrer inactive in the chamber, providing a baseline for comparison with stirred measurements.

The VNA was used to measure the S_{11} parameter of the TEM cell both inside and outside the shielded chamber, with and without the CG present, to evaluate the loading effect. Receiver measurements of the CG were conducted at four different angles: 0°, 90°, 180°, and 270°. At each angle, the CG was tested with and without power, and in each state, the stirrer was activated and deactivated. In a TEM cell, turning the DUT is necessary for accurate measurement because the field generated inside a TEM cell is highly directional, typically aligned along a single axis. Since electromagnetic waves propagate uniformly in one direction, rotating the DUT ensures it is exposed to the field from multiple orientations, capturing how it interacts with the field on all sides. This process provides a comprehensive measurement, as the DUT may behave differently depending on its orientation relative to the field.

In contrast, the reverberation chamber creates a highly reflective environment where the electromagnetic waves bounce around the chamber, creating a statistically isotropic field (uniform in all directions). The superposition of these reflections produces a multi-

directional, randomized field, ensuring that all surfaces and orientations of the DUT are equally exposed without the need for physical rotation. This unique field environment allows for thorough testing in all directions simultaneously, simplifying the process and reducing the need for rotation in order to achieve a complete characterization of the DUT's electromagnetic performance.

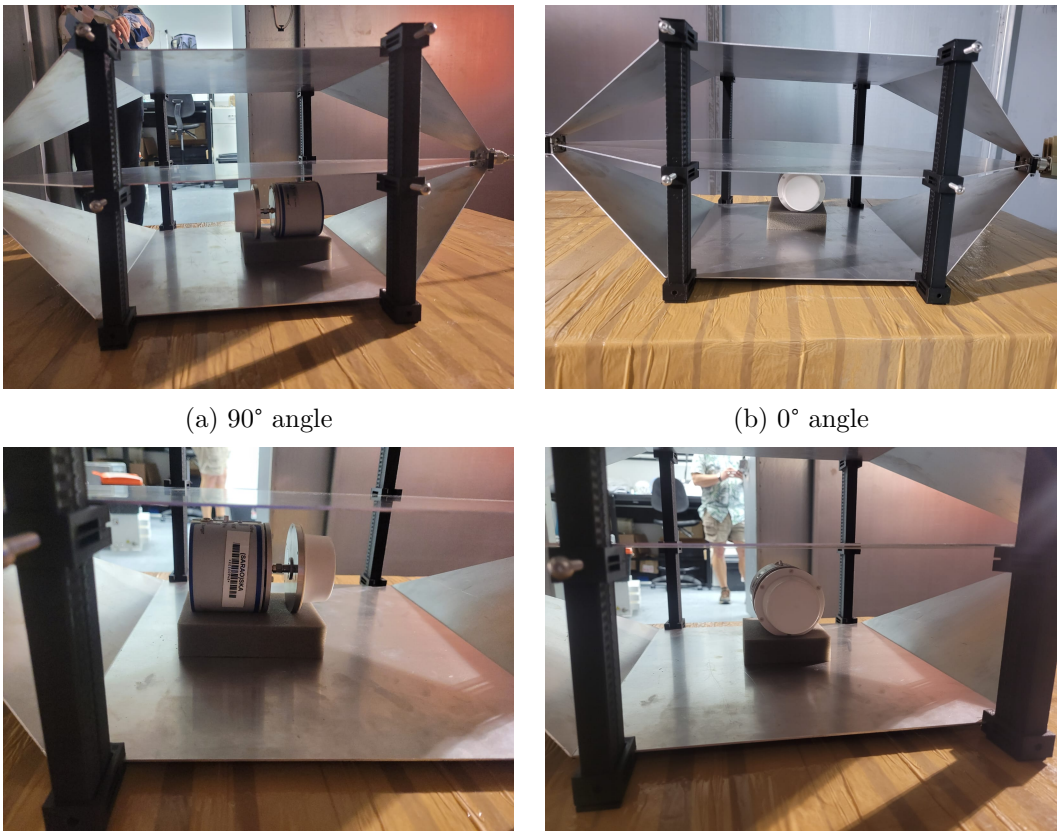

(a) 90° angle

(b) 0° angle

(c) 180° angle

(d) 270° angle

Figure 4.4: Comb Generator Placement Angles

4.4 Measurement Results

This section is divided into specific measurements taken during the testing phase. Each subsection provides a description of the measurement setup and presents the corresponding data.

4.4.1 Comb Generator Measurements in Reverb Chamber

Comb generators emit a unique frequency output that resembles a comb shape, achieved by producing precise frequency intervals. These intervals create distinct spikes on a spectrum analyser, known as comb lines. These lines are expected to be uniform but can vary slightly due to internal electronics. The spacing between spikes is determined by the generator's internal clock rate, usually specified in the device's data sheet. Utilizing a comb generator as a reference signal ensures a stable and predictable frequency pattern, enabling accurate system response evaluation across defined frequency ranges, making it an optimal tool for testing the TEM cell.

First, the generator was placed in the reverberation chamber as shown in Figure 4.5.

Figure 4.5: Comb Generator in Reverberation Chamber

The comb generator was then turned on and the measurement from the reverberation chamber was recorded. The results are shown in Figures 4.5, with the stirrer on and off. The original graph was comb tooth shaped as in figure 4.6. However, the peaks were joined into a line plot for all comb tooth pots for easier readability.

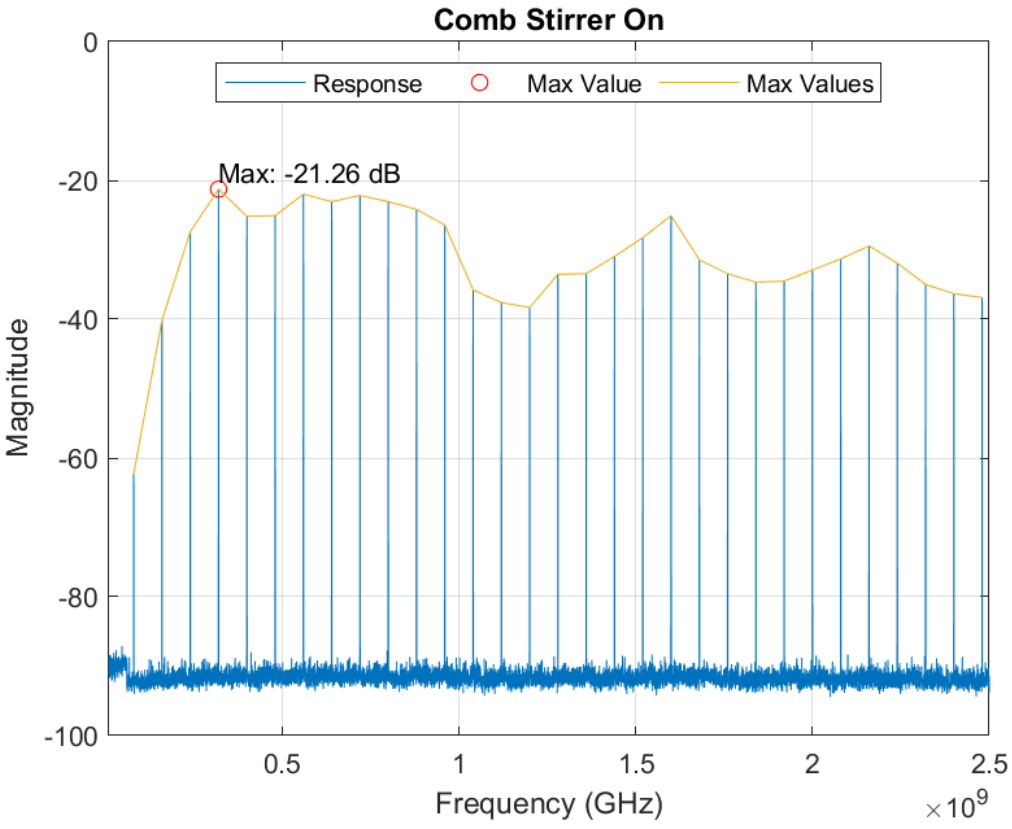

Figure 4.6: Measurement: Reverberation Chamber CG Comb Plot

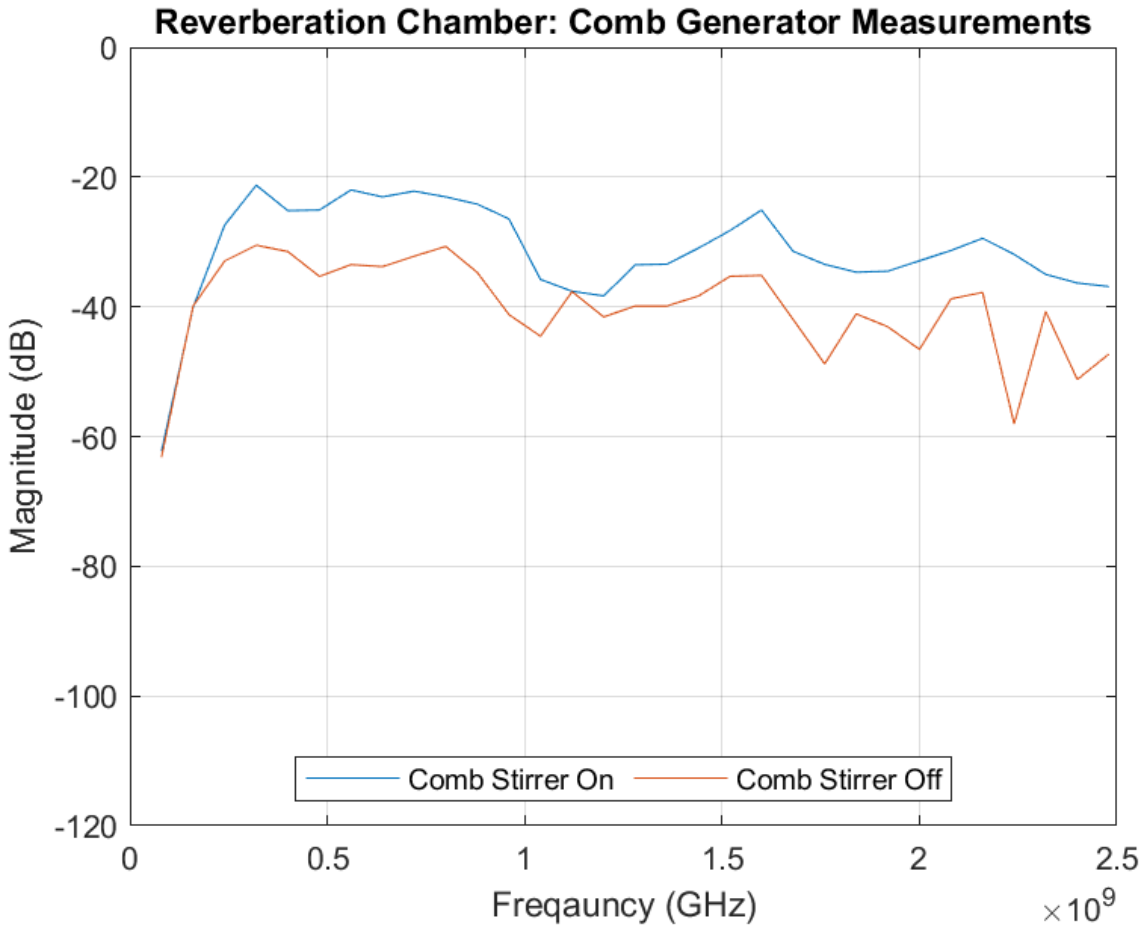

Figure 4.7: Measurement: Reverberation Chamber CG Measurement

With the stirrer in the off state, it can be seen that the comb measured data is equally spaced, although not equal in magnitude. This discrepancy could be due to several factors, such as the internal electronics of the CG, slight reflections in the reverberation chamber, or reflections of the stirrer. However, the results are stable enough to use as a baseline for comparative measurements with the TEM cell to test its performance by comparing the two results. The stirrer was turned on to modify the resonant frequencies within the chamber, providing a more realistic picture of measurements when EMI is present. The difference between the stirrer being on and off is noticeable as expected. Although, without other devices present in the chamber, the overall waveform seems only slightly changed in magnitude, but following the same pattern.

This initial measurement acted as a control to evaluate the measurements made of the CG by the TEM cell. As described in Chapter 4.4, measurements were taken at four different angles: 0°, 90°, 180°, and 270°, set up to assess the impact of the DUT's orientation on test results. For each angle, the receiver was configured with the CG as the DUT, with the chamber stirrer both on and off.

Below are the graphs for the comb generator in each position with the stirrer on and off.

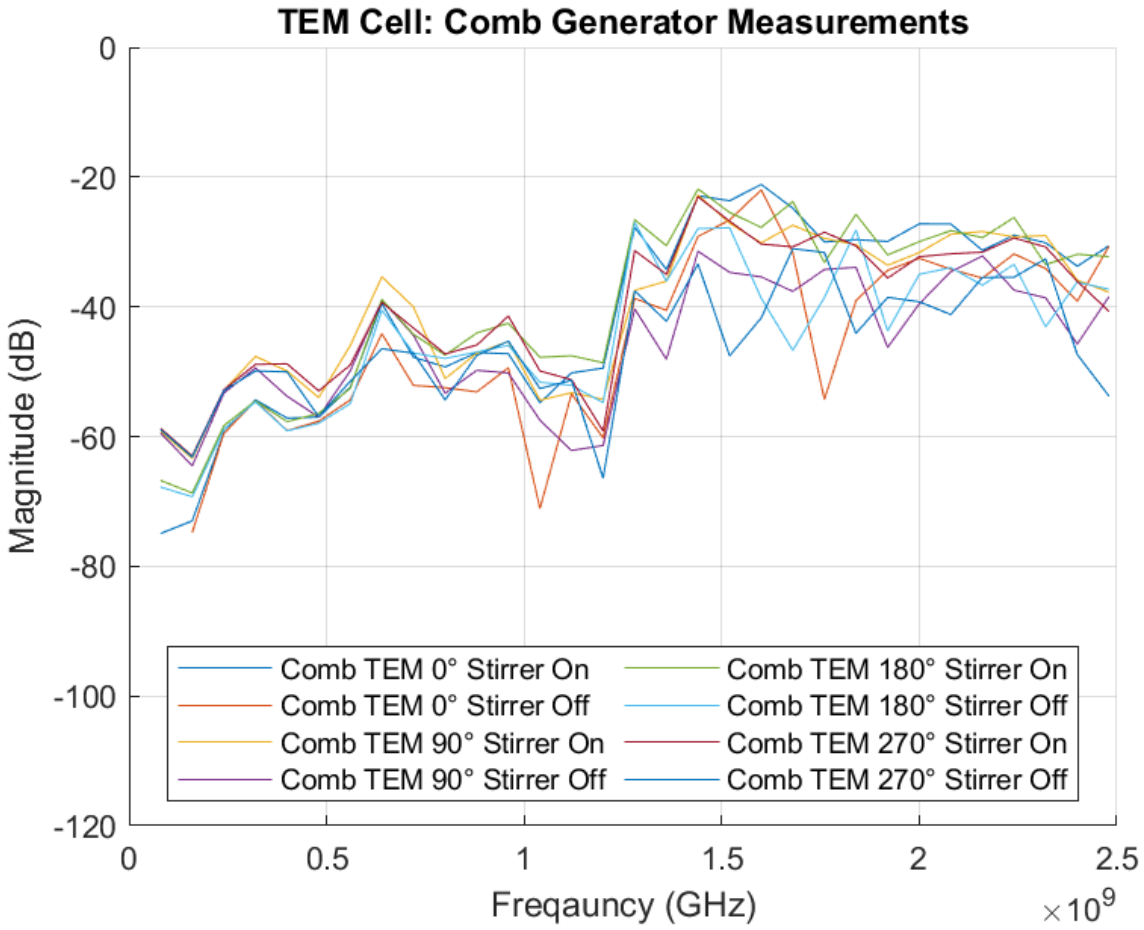

Figure 4.8: Measurement: TEM Cell CG Measurement

Three key observations arise from these results. Firstly, the orientation of the DUT influences the measured readings, underscoring the necessity of varying orientations during testing to ensure comprehensive analysis during the workflow of the CubeSat assembly procedure. This indicates that robust results require multi-angle testing. Consistent results are achieved through orientation variability.

Secondly, the TEM cell demonstrates susceptibility to external noise, evident when the stirrer is activated. Although the waveform remains largely unchanged, the signal magnitude is noticeably affected. Therefore, noise isolation measures should be considered to improve the accuracy of the measurement. This is largely why EMI quiet rooms are best for testing, or closed TEM cells may be preferred to the open type as has been developed. This is, of course, largely dependent on the use case and resource availability. Thus, appropriate noise isolation strategies should be selected based on specific requirements.

Lastly, accuracy varies across frequencies, particularly in lower frequency ranges, where discrepancies from control test results obtained from the reverberation chamber are notable. This analysis is supported by the S_{11} measurements made inside and outside the reverberation chamber.

4.4.2 S_{11} Measurements Inside and Outside the Chamber

Outside Chamber

Two sets of measurements were conducted outside the reverberation chamber using the VNA to evaluate the S_{11} parameter. The first set was taken with the CG active, while

the second set was taken with the CG turned off. The purpose of including measurements with the CG active was to assess the TEM cell's response when the DUT itself is emitting radiated emissions. This allows for evaluating how the presence of emissions from the DUT affects the reflection coefficient and the extent to which the TEM cell can maintain impedance matching under realistic operating conditions. Additionally, it provides insight into how external emissions influence the measurement accuracy in both controlled and noisy environments. The results of these measurements are presented below.

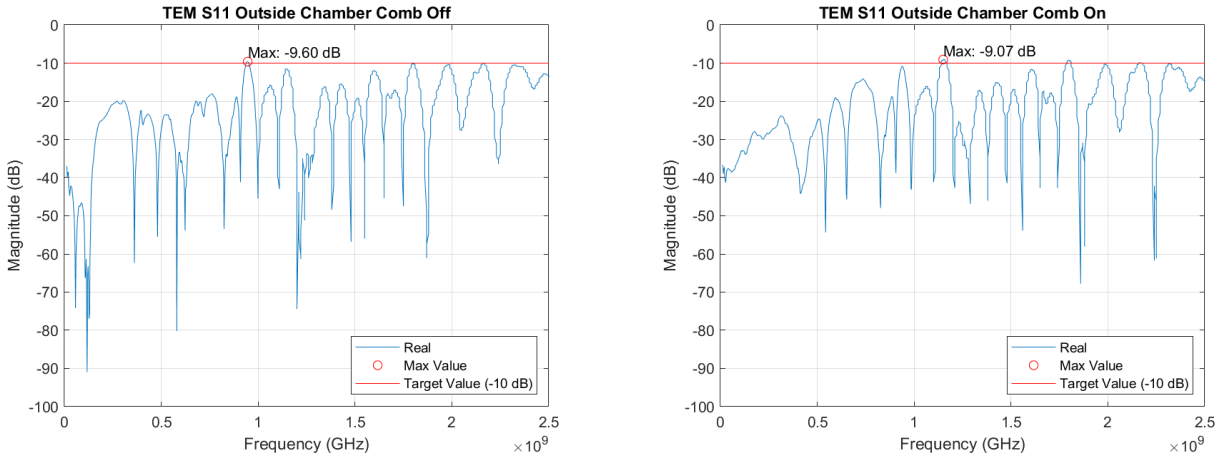

(a) (b)

Figure 4.9: CG TEM Measurement Inside Chamber

The primary objective of the construction was achieved by maintaining a response of less than -10 dB. This was achieved except for a slight deviation around the 1 GHz frequency range. The response exceeded expectations, maintaining below -10 dB beyond 2 GHz, as only a response up to this frequency was simulated.

Even with the CG active, the graph exhibits only a slight shift, but the specified performance criteria were maintained. Based on these results, the next test aimed to evaluate the TEM cell's performance inside the reverberation chamber that the reflections could simulate a noisy environment.

Inside Chamber

Measurements of the S_{11} parameter were also taken inside the reverberation chamber, both with and without the CG active. The data from these measurements are shown below.

It is evident that noise significantly affects the accuracy of the TEM cell in an noisy environment. Not only does the graph exhibit more noise, but the specified performance criteria are not fully met. A significant portion of the graph remains under the -10 dB range, but the graph exhibits a staggering amount of noise. Furthermore the maximum value exceeds -6 dB and that of -10dB at multiple frequencies, whereas in the in the lab outside the reverb chamber, it did not exceed -9 dB. This underscores the importance of using an EMI quiet room or electronics lab on campus for these procedures when testing the DUT to ensure accurate measurements. If such facilities are unavailable, a similar procedure to that followed in this project can be used to design, build, and test a closed TEM cell to achieve better results in a noisy environment.

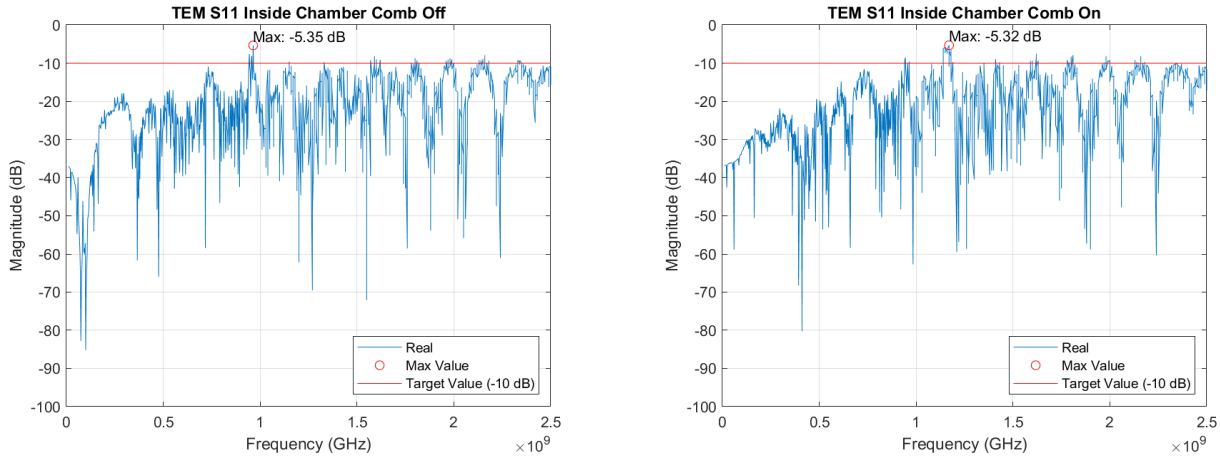

(a) (b)

Figure 4.10: CG TEM Measurement Outside Chamber

Simulation Data

The TEM CELL OPT simulation data, as shown in Figure 3.20, is plotted alongside the measurements taken inside the chamber with the comb generator turned on. The resulting graph is shown below.

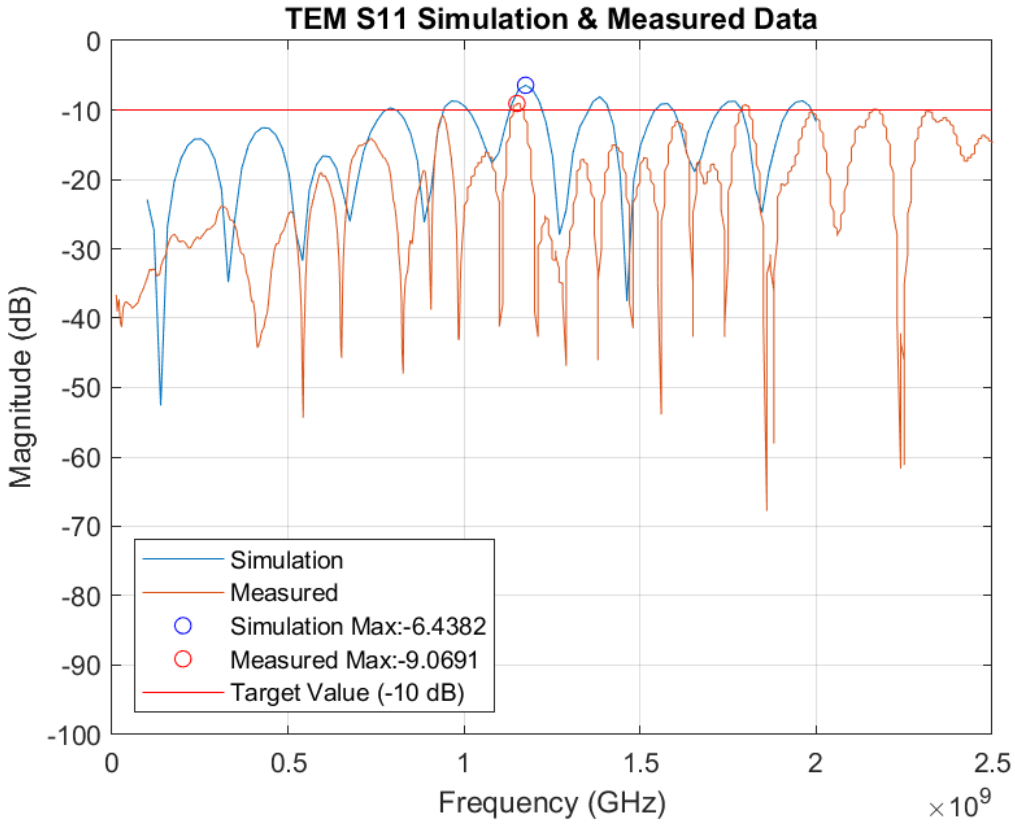

Figure 4.11: TEM Cell Simulation vs. Measured Data

The measured values indicate that the constructed TEM cell performs even better than expected. The observed discrepancy between the simulated and measured results can

largely be attributed to the presence of the CG during measurements, which was not included in the simulation. The comb generator introduces additional loading effects within the TEM cell, impacting the measured S_{11} response. While minor inaccuracies in simulating the N-type connector could contribute to differences, the dominant factor is likely the difference in loading conditions between the simulation and the physical test.

Despite this, the TEM cell performs well within allowable parameters, with most measured values below the -10 dB threshold and closely matching the peaks and valleys of the simulated data, especially in the upper frequency range. This demonstrates the developed procedure's effectiveness and its likely repeatability (**RQ3 p.11**).

Chapter 5

Discussions

5.1 Implications for CubeSat Subsystems

5.1.1 Increased Usable Test Area

The TEM cell emerged as a crucial element in EMC pre-compliance testing for many organizations. However, the demand for higher frequencies necessitated smaller transmission structures to achieve uniform field distribution, leading to the introduction of higher-order modes. The usable test area of commercial TEM cells for 900 MHz frequencies was limited to 20 mm. The objective was to expand this area to approximately 90 mm while retaining testable frequencies within the range of DC to 2 GHz and maintaining a characteristic impedance of 50 Ω. The size of the TEM cell was vital to preserve the integrity of the homogeneous EM field during testing. Despite being broadband with a linear phase and amplitude response from DC to the cell's cut-off frequency, the upper useful frequency was constrained by the cell's physical dimensions, subsequently limiting the size of the Device Under Test (DUT).

Besides the aforementioned design considerations, various other factors can influence TEM cell design. These include composition, performance, principles, analysis and calculation, simulation, and surface treatment, all of which contribute to meeting design requirements.

5.2 Recommendations

5.2.1 TEM Cell Measurements

When conducting measurements using a TEM cell, it is imperative to address several factors to ensure accuracy.

Mitigating Ambient Noise Utilizing an open TEM cell may lead to the detection of ambient noise signals. To mitigate this issue, tests should be performed in an EMI quiet room.

Addressing the Noise Floor Emissions from the DUT in TEM cells might occasionally fall below the noise floor displayed on a spectrum analyser, posing a common challenge. To improve detection, inserting a preamplifier with a gain of approximately 20-40 dB between the TEM cell and the spectrum analyser can be beneficial. However, this approach carries the risk of damaging the analyser.

RF Connection: Ensure proper coaxial cable connection to the signal generator or spectrum analyser, depending on the type of EMC testing being conducted. Secure connections minimize signal loss and leakage.

Outer Shield: Verify the secure attachment of the two grounded plates, visible on the triplate TEM cell, to the coaxial cable shield. This step ensures proper grounding and eliminates stray electromagnetic interference.

DC Block: Consider employing a DC block with an appropriate voltage rating to safeguard the analyser's sensitive input from inadvertent DC voltage application, providing essential protection to the instrument.

Septum Inspection: Regularly inspect the septum for any indications of damage or wear. A compromised septum can affect signal integrity and measurement accuracy.

50 Ohm Load: Ensure proper termination with a 50 Ohm load to prevent signal reflections within the cell, thereby averting inaccurate readings and error introduction.

Noise Reduction: Additionally, to further diminish noise during measurements, contemplate enclosing the TEM cell within an Electromagnetic Compatibility (EMC) bag. This shielding will protect the cell from external electromagnetic interference, improving the signal-to-noise ratio and overall measurement accuracy.

Figure 5.1: TEM Cell Shield Bag

Reflection Coefficient: When evaluating the reflection coefficient, any frequencies that appear out of range may indicate the presence of standing waves. Further analysis can help identify specific problematic areas on the septum, where small isolators—such as the black dots on the septum—can be strategically inserted to mitigate these effects (**RQ11 p.12**). See figure 5.2

Figure 5.2: Septum Isolators

Chapter 6

Conclusion

In conclusion, this research demonstrates that a TEM cell suitable for EMC pre-compliance testing of CubeSats can be successfully fabricated using in-house resources and dedicated machinery. The methodology applied in this study—relying on student-driven efforts and campus facilities—highlights the feasibility for academic institutions to independently develop specialized EMC testing equipment. This approach is advantageous not only for its cost-effectiveness and precision but also for its educational value, as it provides students with hands-on experience in building their own EMC analysis tools.

With the devolved TEM cell having a cost of R3 500.00 the TEM cell's design criteria offer clear advantages over larger anechoic and reverberation chambers, not only in cost but also in terms of floor space requirements. While larger chambers can measure much higher frequencies with greater accuracy, they are impractical for the requirements outlined in this project, making the TEM cell the more suitable choice (**RQ8 p.12**).

The process encompassed design considerations, material machining, and comprehensive simulation-based optimization. The resulting TEM cell met the desired specifications, achieving a stable 50 Ω impedance across the designated frequency range, with acceptable deviations suitable for pre-compliance testing requirements. Additionally, the use of a custom-built PCB septum—unique to this study—provided flexibility and customization to address specific testing needs.

Moreover, the project underscored the value of collaboration among engineering students, researchers, and technicians, illustrating how academic settings can foster both innovation and practical skill development. The successful development of this TEM cell for EMC testing reaffirms the capability of educational institutions to advance EMC compliance testing for CubeSat technologies. This project marks a significant step forward in promoting EMC research and addressing compliance needs in the growing field of miniaturized satellites for the space industry.

References

Academy of EMC (2020). *Electromagnetic Compatibility In A Nutshell*. URL: https://www.academyofemc.com/emc-in-a-nutshell (visited on 10/10/2020).

Al Takach, Ali et al. (2018). "3D-Printed Low-Cost and Lightweight TEM Cell". In: *2018 International Conference on High Performance Computing Simulation (HPCS)*, pp. 47–50. DOI: 10.1109/HPCS.2018.00022.

Altair University (Jan. 5, 2021). *Altair Feko*. Version 2021-3913. URL: https://altairuniversity.com/feko-student-edition/.

Arezoomand, Masoud, Mohsen Kalantari Meybodi, and Narges Noori (2016). "Design of a TEM cell using both multi-step and piecewise linear tapering". In: *2016 8th International Symposium on Telecommunications (IST)*, pp. 571–574. DOI: 10.1109/ISTEL.2016.7881886.

Armstrong, Keith (1999). *EMC for Systems and Installations*. Newnes.

Autodesk (May 11, 2021). *Autodesk Inventor*. Version 2021.3.1. URL: https://www.autodesk.co.za/.

Bentz, S. (1996). "Use of the TEM cell for compliance testing of emissions and immunity, an IEC perspective". In: *Proceedings of Symposium on Electromagnetic Compatibility*, pp. 43–47. DOI: 10.1109/ISEMC.1996.561198.

Boyce, Aphiwe (Apr. 24, 2021). *Maritime Domain Awareness Satellite mission launch imminent*. URL: https://www.cput.ac.za/newsroom/news/article/4201/maritime-domain-awareness-satellite-mission-launch-imminent (visited on 2021).

Crawford, M.L. and J. L. Workman (1979). *Using a TEM Cell for EMC Measurements of Electronic Equipment*. Vol. 1013. NATIONAL BUREAU OF STANDARDS.

Crawford, Myron L. (1974). "Generation of Standard EM Fields Using TEM Transmission Cells". In: *IEEE Transactions on Electromagnetic Compatibility* EMC-16.4, pp. 189–195. DOI: 10.1109/TEMC.1974.303364.

Diamond Systems (Apr. 18, 2021). *Perfect-Fit Solutions*. URL: http://www.diamondsystems.com/aboutus/perfectfit.php (visited on 2021).

Eadie, Andy (2019a). *TekBox Compact TEM Cell (TBTC1)*. URL: https://www.emcfastpass.com/test-equipment/shop/gtem-tem-cells/compact-tem-cell-tbtc1/ (visited on 06/01/2024).

– (2019b). *TekBox Medium TEM Cell (TBTC2)*. URL: https://www.emcfastpass.com/test-equipment/shop/gtem-tem-cells/midsize-tem-cell-tbtc2/ (visited on 06/01/2024).

– (2019c). *TEM Cell and GTEM Guide For Radiated Emissions & Radiated Immunity Pre-Compliance Testing*. URL: https://emcfastpass.com/tem-cell-guide/ (visited on 03/03/2021).

EMC Learn (2020). *Learn EMC. Introduction to EMC*. URL: https://learnemc.com/introduction-to-emc (visited on 08/17/2020).

European Space Agency (Sept. 5, 2012a). *ECSS-E-HB-20-07A – Electromagnetic compatibility handbook (5 September 2012). European Cooperation for Space Standardization.*

European Space Agency (Feb. 12, 2012b). *ECSS-E-ST-20-07C Rev.1 – Electromagnetic compatibility (7 February 2012). European Cooperation for Space Standardization.*

F'SATI (Apr. 18, 2021a). *ZACUBE-1.* URL: https://blogs.cput.ac.za/fsati/zacube-1/# (visited on 2021).

– (Apr. 18, 2021b). *ZACUBE-2.* URL: https://blogs.cput.ac.za/fsati/zacube-2/ (visited on 2021).

Hariyawan, Y, R S Darwis, and B A Habibi (Feb. 2024). "The Statistical Field Uniformity Criterion in Transverse Electromagnetic Waveguides". In: 1073.1, p. 2052. DOI: 10.1088/1757-899x/1073/1/012040.

Ho, Tzu-Hao et al. (2019). "Design and Characteristic Calibration of TEM Cell for IC Radiation EMC Test". In: *2019 Electrical Design of Advanced Packaging and Systems (EDAPS)*, pp. 1–3. DOI: 10.1109/EDAPS47854.2019.9011660.

IEEE Std 1302-2019 (2020). "IEEE Guide for the Electromagnetic Characterization of Conductive Gaskets in the Frequency Range of DC to 40 GHz - Redline". In: *IEEE Std 1302-2019 (Revision of IEEE Std 1302-2008) - Redline*, pp. 1–103.

Malaric, K. and J. Bartolic (203). "Design of a TEM-Cell with Increased Usable Test Area". In: *Turk J Elec Engin* 11.2, pp. 143–154.

MathWorks (Mar. 1, 2021). *MathWorks Matlab.* Version 9.10. URL: https://www.mathworks.com/.

Media, Hughes (2020a). *EMC Standards. Lightbulbs and Set Boxes.* URL: https://www.emcstandards.co.uk/lightbulbs-and-set-top-boxes (visited on 11/10/2020).

– (2020b). *EMC Standards. When the railway interfered with the Large Hadron Collider.* URL: https://www.emcstandards.co.uk/home (visited on 11/10/2020).

Paul, Clayton R (2006). *Introduction to electromagnetic compatibility.* Vol. 184. John Wiley & Sons. Chap. 1.1 Aspects of EMC.

Pozar, David M. (2012). *Microwave Engineering.* Vol. 4. John Wiley & Sons, Inc. Chap. 3.7.

R.D. Leach, M.B. Alexander (1995). "Electronic Systems Failures and Anomalies Attributed to Electromagnetic Interference". In: 1374, p. 5.

Rocker Lab USA (2020). *Space Is Open For Business, Online.* URL: https://www.rocketlabusa.com/about-us/updates/space-is-open-for-business-online/ (visited on 12/21/2020).

Sandeep M. Satav, Vivek Agarwal (2008). "Do-it-Yourself Fabrication of an Open TEM Cell for EMC Pre-compliance". In: pp. 66–71.

Sibanda, M. and R. Ryk Van Zyl (2016). "Practical electromagnetic compatibility studies of a CubeSat". In: 14.4, pp. 770–780.

Space, AAC Clyde (2023). *Optimus Battery.* URL: https://www.aac-clyde.space/wp-content/uploads/2021/10/AAC_DataSheet_Optimus.pdf (visited on 2023).

Tekbox Digital Solutions (2020). *MANUAL: OPEN TEM CELLS FOR EMC PRE-COMPLIANCE TESTING.* URL: https://www.tekbox.com/product/open-tem-cells-emc-compliance-testing/ (visited on 03/03/2021).

TheEMCShop (2024a). *Tekbox open TEM cell TBTC1.* URL: https://theemcshop.com/anechoic-chambers/used-semi-anechoic-emc-test-chamber-3-meter/ (visited on 06/01/2024).

– (2024b). *Used Fully Anechoic 3 Meter EMC Test Chamber.* URL: https://theemcshop.com/anechoic-chambers/used-fully-anechoic-3-meter-emc-test-chamber/ (visited on 06/01/2024).

– (2024c). *Used Semi-Anechoic EMC Test Chamber - 3 Meter.* URL: https://theemcshop.com/anechoic-chambers/used-semi-anechoic-emc-test-chamber-3-meter/ (visited on 06/01/2024).

Yıldız Cemil Demirel Gülsima, Çalışkan Fatma (n.d.). "Designing Transverse Electromagnetic (TEM) Cell". In: (), pp. 1–4.

Appendix A

Appendices

A.1 Appendix A: Datasheets

Data Sheet

HUBER+SUHNER

Coaxial Panel Connector
23_N-50-0-1/133_N

Description

Straight panel receptacle jack, flange mount

Interface standards
IEC 61169-16_MIL-STD-348A/304_CECC 22210

Technical Data

Electrical Data

Impedance	50 Ω
Interface frequency max.	11 GHz

Mechanical Data

Number of matings	500
Weight	0.0301 kg

Environmental Data

Operating temperature	-65 °C to 165 °C
2011/65/EU (RoHS - including 2015/863 and 2017/2102)	compliant

Material Data

Piece Parts	Material	Surface Plating
Centre contact	Bronze	Gold Plating (Nickel underplated)
Outer contact	Brass	SUCOPLATE (R) Plating
Body	Brass	SUCOPLATE (R) Plating
Insulator	PFA / PTFE	

Related Documents

Outline drawing	DOU-00010382
Catalogue drawing	DCA-00010384
Mounting hole	DOU-00010096

Ordering Information

Single package	23_N-50-0-1/133_NE

23 N 50 - 0 - 1 ML 17

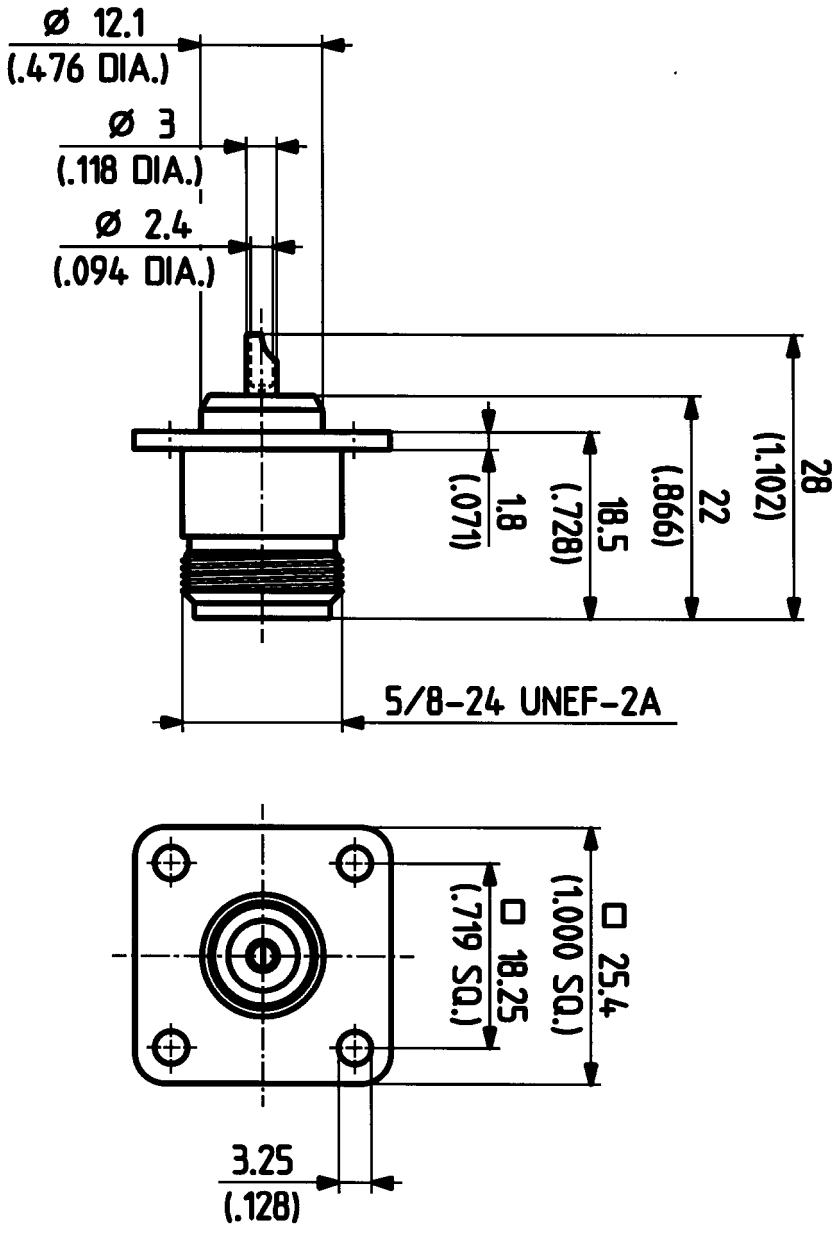

	Datum	Kurzz/Visum
Erstellt	02.02.96	023/Tu[illegible]
Geprüft	[illegible]	[illegible]
Freigabe	[illegible]	[illegible]

M. 2:1

HUBER + SUHNER AG
9100 Herisau

3.13.0334.0_1 b

webb
A JASCO COMPANY

DC— - 3000 MHz

LOAD TERMINATIONS

- ☑ This 75 W coaxial load resistor provides a stable 50 Ohm termination and an extremely low VSWR required by circulators and hybrids..
- ☑ It is designed to absorb reflected power when used in conjunction with isolators.
- ☑ It can also be used to terminate unused ports in combiner systems.

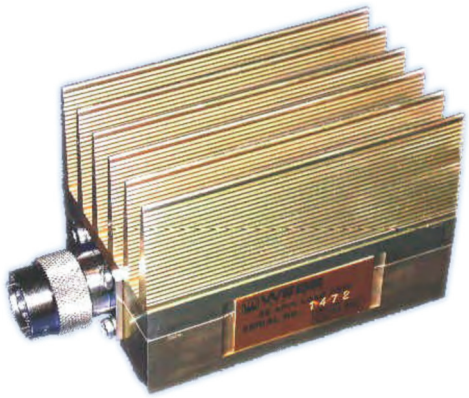

ALE075

D10AA0082A (N) / D10AA0524A (DIN 7/16)

Electrical Data	**ALE075**	
Frequency	DC—3000 MHz	
Power Rating	65 W @ 40°C, 75 W @ 25°C	
VSWR (max)	1,15 : 1 (max)	
Impedance	50 Ohm	
Termination Type	N male	7/16 DIN male
Mechanical Data		
Temperature Range	-40 to 40°C	
Coolant	Dry (Convectional Cooling)	
Length	115 mm	
Width	56 mm	
Height	65 mm	
Packed Weight	0,5 kg	

www.webb.co.za
webb@webb.co.za
tel .....+27 11 719-0000
fax ....+27 11 444-2288

JASCO INSPIRE.INNOVATE.